Joint Experimental/Theoretical Investigation of the Chemoselective Iridium(III) Metallacycle-Catalyzed Reduction of Substituted γ-Lactams by Et3SiH

Halima Khadraoui, Chunchesh Malangi Gajendramurthy, Sara Figueirêdo de Alcântara Morais, Yann Cornaton, Hédi M'rabet, Philippe Bertani, Aïcha Arfaoui, Jean-Pierre Djukic

Joint Experimental/Theoretical Investigation of the Chemoselective Iridium(III) Metallacycle-Catalyzed Reduction of Substituted γ-Lactams by Et_3SiH

Halima Khadraoui,[a,b] Chunchesh Malangi Gajendramurthy,[b] Sara Figueirêdo de Alcântara Morais,[b] Yann Cornaton,[b] Hédi M'rabet,[a] Philippe Bertani,[b] Aïcha Arfaoui[a,*] and Jean-Pierre Djukic,[b,*]

[a]Université de Tunis El Manar, Faculté des Sciences de Tunis, Laboratoire de Synthèse Organique Sélective et Hétérocyclique-Evaluation de l'Activité Biologique, 2092 Tunis, Tunisie.

[b]Institut de Chimie de Strasbourg, CNRS UMR 7177. Université de Strasbourg. 4 rue Blaise Pascal F-67000 Strasbourg, France.

Supporting Information Placeholder

ABSTRACT: This study addresses the chemoselectivity of the catalyzed reduction of a series of variously substituted γ-lactams by Et_3SiH mediated by a pentamethylcyclopentadienyl iridacyclic acetonitrilo salt derived from benzo[*h*]quinoline. Introduction of an unsaturation within the 5-membered ring of the γ-lactam annihilates the precedence of the amide function over the capture of the silylium cation, which results in a lower chemoselectivity. Monitoring over time the catalyzed reduction of a γ-lactam bearing a carboxylic ester appendage by ^1H NMR spectroscopy revealed pseudo–zero order kinetics for the prior hydrosilylation of the lactam's amide. This primary hydrosilylation reaction is followed by the full conversion of the formed intermediate into a pyrrolidine following a pseudo-first-order rate law. Under anhydrous conditions, the hydrosilylation of the pendant ester function occurs only in a late stage once the γ-lactam's amide function has underwent full reduction of the carbonyl function. DFT investigations show that chemoselectivity is 1) governed by the affinity of the organic substrate for the triethylsilylium cation produced by the electrophilic activation of Et_3SiH by the Ir(III) catalyst and 2) by the ability of the *in situ*-formed hydrido-iridium(III) intermediate to transfer hydride to the activated substrate.

INTRODUCTION

The elaboration of selective and performant methods for the synthesis of pyrrolidines is of major importance, since they represent significant building blocks for polymers and dyes.[1] Pyrrolidines are common structural motives in biologically active plant alkaloids,[2] and hence, convenient, and selective methods for their design are especially valued for by the pharmaceutical industry[2-3] (Figure 1).

The synthesis of pyrrolidines by the reduction of lactams requires a good control of the chemoselectivity of the process particularly if multiple competing functions are present in the starting lactam. Hydrides such as $LiAlH_4$[4] and B_2H_6 or other boranes[5] have long offered the most atom-efficient methods of reduction. Current established procedures suffer from low selectivity and relatively harsh reaction conditions, though, which commend the development of milder and more selective alternative methods.[6] Catalytic strategies are expected to provide more convenient methods for selective reductions, offering increased chemo- and regioselectivity.[7]

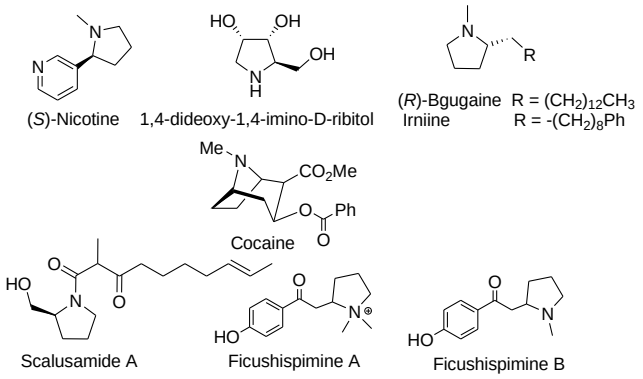

Figure 1. Chemical structures of some biologically active pyrrolidine alkaloids and their derivatives.

Transition-metal-complex-catalyzed reductive reactions using hydrosilanes have recently emerged as highly desired procedures for the aliphatic and heterocyclic amides reduction.[8] Hydrosilanes are particularly attractive reducing agents due to their ease of handling and storage, chemical stability over time

and moderate to low toxicity. Numerous procedures have been developed for the catalytic hydrosilylation of amides based on noble metals.[9] Metal-catalyzed hydrosilylation[10] reactions of C-C and heteroatom unsaturated compounds have been subject to intensive research and represents an active field of investigation and development. Nonetheless, one challenging issue is that of chemoselectivity[11] of the hydrosilylation catalysis in the synthesis of polyfunctional biorelevant molecules. At first, it is expected that the outcome of hydrosilylation reactions on such substrates possessing several competing sites of reaction depends on the reactivity of the various organic functions as well as on the way the hydrosilane is itself activated by the metal-based catalyst.

Mainly two modes of activation of hydrosilanes can be commonly encountered and achieved that have different consequences on the interaction with the substrate.[12] The Si-H bond may either undergo oxidative-addition at the catalyst's metal center or the electrophilic cleavage[13] of the bond resulting into the transfer of the hydride to the metal and into the capture of the formed silylium cation[14] by any Lewis base, including one or several at the substrate. While the oxidative pathway requires the organic unsaturated substrate to directly interact with the metal center to undergo further reaction, the electrophilic activation pathway reduces the whole question of the selectivity of the reductive hydrosilylation reaction to the competition between various Lewis basic sites present at the substrate for capturing the generated highly electrophilic $[SiR_3]^+$ silylium cation.[14d,14e] 2-Phenylpyridine and benzo[*h*]quinoline-derived[15] iridium(III)-based metallacycles are efficient hydrosilylation catalysts that operate by the electrophilic Si-H bond activation pathway; both the neutral and cationic variants of these organoiridium complexes have shown outstanding efficiency in the hydrosilylation of a great variety of organic functions such as alkenes, alkynes, amides, ketones and aldehydes and nitriles.[10a,10b,10d-f,13b,14a,14b,15-16] In the present study a cationic acetonitrilo iridium complex [**Ir-NCMe**]$BArF_{24}$ (scheme 1) is used that requires no activating cocatalyst and possesses an outstanding reactivity with organic unsaturated functions such as in nitrile compounds R-CN.[14a,14b,15]

Scheme 1. Synthesis of pyrrolidines by the Ir(III)-catalyzed reduction of γ-lactams

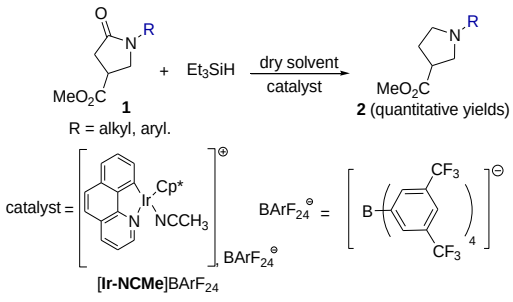

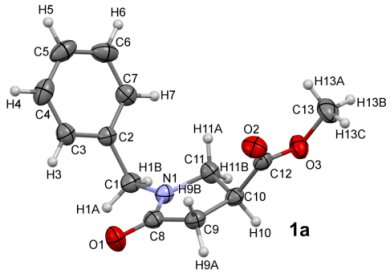

Figure 2. ORTEP drawing of the structure of compound **1a** resolved by X-ray diffraction analysis drawn at the 50% probability level (*Si* face of the amide's carbonyl on top of the 5-membered ring).

Scheme 2. Pyrrolidin-2-ones synthesized for the purpose of the present study.

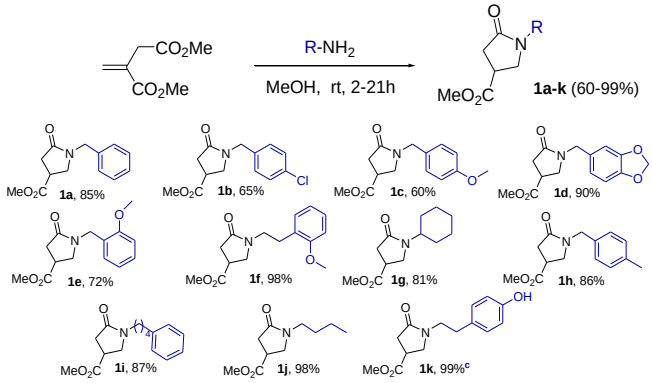

The application of an easily accessible iridium (III) metallacycle to the promotion of a one-pot simple or sequential double hydrosilylation of lactams **1** and other structural analogues, addressing a chemoselective approach to the related pyrrolidines **2** (scheme 1) by the catalyzed reduction of the former lactams, is disclosed and discussed herein.

RESULTS AND DISCUSSION

The pyrrolidin-2-ones **1** (schemes 1 and 2) were synthesized following an established route.[17] The Michael addition of a series of primary amines to commercially available dimethyl itaconate in methanol at room temperature under anaerobic Schlenk technique conditions afforded the functional pyrrolidin-2-ones in yields >65%; the reaction being compatible with aliphatic substituents, aromatic and hetero-aromatic benzene rings. This study was started using *methyl 1-benzyl-5-oxopyrrolidine-3-carboxylate* **1a** (Figure 2) as a model substrate to optimise the reaction conditions (Table 1). Notably, the structure of **1a** (Figure 2) displays rather accessible amide and ester functions over which the benzyl group operates only little steric cluttering: the amide function appears slightly more sterically cluttered on its *Si* face than its *Re* one, a minor feature that did not interfere in the catalysis as shown farther.

In general, the reaction proceeded smoothly with Et_3SiH (1 to 6 equivalents) used as the reducing agent and [**Ir-NCMe**]$BArF_{24}$ as the catalyst in all the reactions reported therein. Different solvents, such as THF, $CDCl_3$, CH_2Cl_2 (abbr. DCM) and CD_2Cl_2, and 1,2-dichloroethane (abbr. DCE)

were investigated as to their adequacy in this catalysis. It was found that DCE was particularly suited to the optimal conditions affording quantitative yields (Table 1, entry 11) compared to other chlorinated solvents of low coordinating ability (DCM and $CDCl_3$), which all would require sealed vessels to allow reactions to run for hours above the respective boiling points at normal pressure (Table 1, entries 13 and 7). Noteworthy, under identical conditions THF proved to be significantly detrimental to the performance of the reaction providing only 40% yield in **2a** at 60°C (Table 1, entry 12).

Table 1. Optimization studies for the reduction of pyrrolidin-2-one 1a with Et_3SiH catalyzed by iridium catalyst. [a]

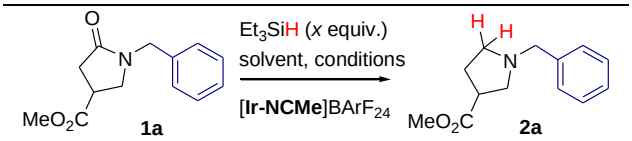

entry	Et_3SiH (*x* equiv.)	solvent	time (h)	temperature (° C)	yield[b] in **2a**
1	1	DCE	22	25	0
2	2	DCE	22	25	47[c]
3	2	DCE	5 days	25	31[c]
4	2	DCE	5	40	44 [d]
5	2	DCE	75	40	30[d]
6	6	DCE	6 days	40	80[d]
7	2	$CDCl_3$	5	50	0[e]
8	2	$CDCl_3$	22	50	18[e]
9	3	DCE	15	60	43[g]
10	6 (3+3[f])	DCE	40	60	100[g]
11	6	DCE	4	60	100
12	6	THF	4	60	40
13	6	DCM	2	25	40

[a]Reaction conditions: the reactions (entry 1 to 13) were carried out with 0.08 mmol of **1a**, 5 mol % of Ir catalyst, *x* (equiv.) of Et_3SiH in 2 mL of solvent under an argon atmosphere. [b]yield determined by ^1H NMR spectroscopy. [c] The ^1H NMR spectrum collection was carried out from the same reaction mixture after 22 h and 5 days. [d] The ^1H NMR spectrum was obtained from the same reaction mixture after 5 h, 75 h and 6 days. [e] The ^1H NMR spectrum was collected from the same reaction mixture after 5 h and 22 h. [f] 3 equiv. of Et_3SiH were added to the mixture of entry 9 after 15 h of stirring at 60 °C. [g] the ^1H NMR spectrum was acquired after 15 h then 40 h. Note that the formation of **2a'** was never observed under the experimental conditions of these runs.

All reactions were performed optimally with 5 mol% of Ir(III) catalyst and excess of Et_3SiH with excellent chemoselectivity (entries 1 to 13), that is with no side formation of **2a'** (scheme 3), i.e. the product of hydrosilylation of the ester function of **2a** that was observed only when the reaction was carried out in a sealed J-Young NMR sample tube under strict anhydrous and anaerobic conditions (*vide infra*).

The mode of activation of Et_3SiH by [**Ir-NCMe**]$BArF_{24}$ entails the electrophilic cleavage of the H-Si bond in Et_3SiH like shown in scheme 3 leading to the trapping of the silylium moiety by the formed hydrido-iridium species [**IrH**] to form the labile [**IrH(Si)**]$^+$ intermediate[14b] from which the $[Et_3Si]^+$ moiety can be abstracted by any stronger Lewis base present in the medium. The latter is in great part responsible for the observed chemoselective reduction of the amide function in **1a**, which seems to be guided by the discriminating affinity of $[Et_3Si]^+$ for the most Lewis basic site in **1a**, *i.e.* the lactam's amide O atom (*vide infra*).

No competing hydrosilylation of the more sterically accessible ester function is observed in the early stages of the catalysis. The capture of the silylium by the lactam's amide O atom, raises the electrophilic character of the lactam's amide and opens the reactive channel for the hydride transfer from the key hydrido-iridium intermediate [**IrH**]. This putatively leads to a highly reactive transient silyloxy intermediate that is further displaced by a hydride upon prior activation of the silyloxy group by $[Et_3Si]^+$.

Scheme 3. Proposed mechanism of catalyzed reduction of the amide function of 1a.

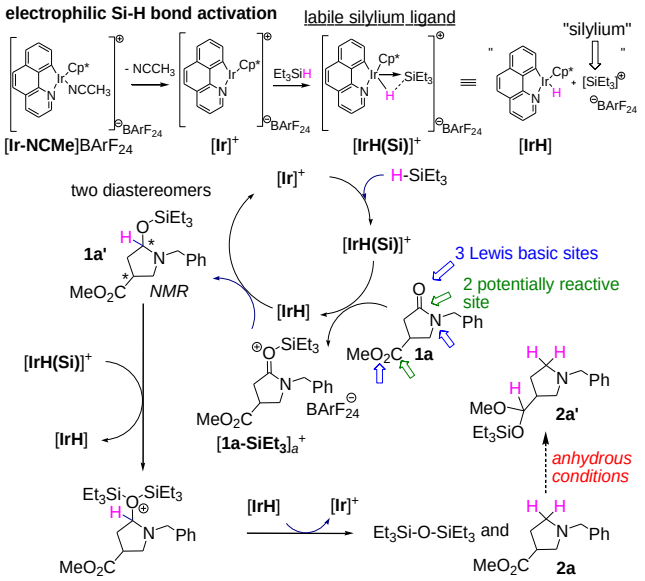

This central role of the silylium species also stresses the importance of the anhydricity of the medium as a key experimental requirement that is seemingly difficult to achieve or preserve over time with standard Schlenk techniques. It must be pointed out that the successful reduction of the amide function of the lactam into a cyclic amine such as **2a** requires the crucial electrophilic centers at the heterocycle to be sterically accessible by the hydrido-iridium [**IrH**] species. Any steric cluttering would result in an increase of the concentration of "idle" silylium species hanging at Lewis bases, leading either to its decomposition or to its migration to any alternative Lewis base, thus reducing not only the yield of the desired reaction but also its chemo- and regioselectivity.[15]

The iridium catalyst [**Ir-NCMe**]$BArF_{24}$ (5 mol%) promotes the reduction of a variety of pyrrolidin-2-ones (cyclic amides) **1a-k** (scheme 2) by Et_3SiH at 60 °C of DCE (Table 2). The reduction was shown to be compatible with aliphatic, aromatic and hetero-aromatic substituents to produce the corresponding pyrrolidines **2a-j** (cyclic amine) in excellent yields. Methoxy and dioxomethylene groups in **2c-f** are interestingly left untouched by the catalysis.

Only in the case of the 4-hydroxyphenyl substituted **1k** was a conversion of the hydroxy group into the silylether **2k** observed along with the product of the ester hydrosilylation of **2k**, i.e. **2k'**.

Table 2. Synthesis of pyrrolidines 2a-k by the catalyzed reduction of pyrroldin-2-ones 1a-k [a]

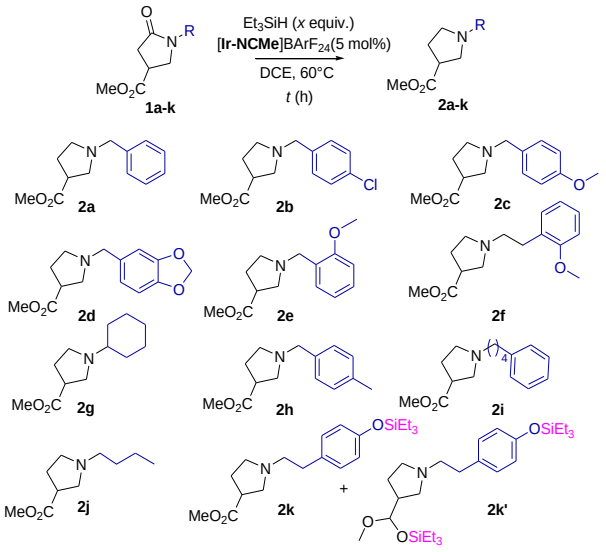

entry	product	Et_3SiH (*x* equiv.)	time (h)	yield (%)
1	**2a**	6	4	99 [b]
2	**2b**	8	12	98 [b]
3	**2c**	8	24	99 [b]
4	**2d**	20	38	98 [b]
5	**2e**	8.5	32	93 [b]
6	**2f**	9	10	87 [b]
7	**2g**	25	44	75 [b]
8	**2h**	4	30	99 [b]
9	**2i**	4	7	100 [b]
10	**2j**	6	18	94 [c]
11	**2k+2k'**	18	16	100 [c]

[a] Reaction conditions: the reaction was carried out with 30 mg of **1a-k**, 5 mol% of Ir catalyst, *x* equiv. of Et_3SiH in 3 mL of DCE under an atmosphere of argon at 60°C. [b] Isolated yields after purification using flash column chromatography. [c] Determined by ^1H NMR spectroscopy.

Catalyzed reduction of methyl 1-benzyl-5-oxo-4,5-dihydro-1H-pyrrole-3-carboxylate with Et_3SiH. To further probe the chemoselectivity of the catalytic system a limited series of γ-lactams **4a-c** (Figure 3) was synthesized (scheme 4). The synthesis was carried out in a three-step sequence consisting of two successive nucleophilic reactions of the primary amine (2 equiv.) in boiling bromobenzene to give an isomerisation intermediate, which, after a 5-exo-trig cyclization, spontaneously afforded the cyclic enamides **4a-c** in yields spanning 50-70%. As shown in Figure 3 the planarity of the 5-membered rings makes the amide's carbonyl equally accessible on both *Si* and *Re* sides as compared to **1a** (Figure 2). Quite surprizingly, the Ir(III) catalyst (5 mol%) was found to promote exclusively the reductive *endo*-to-*exo*cyclic double bond isomerization of cyclic enamides **4a-c** with Et_3SiH at 60°C in DCE, into new pyrrolidin-2-ones **5a-c** containing an exocyclic double bond of an enol silyl ether in moderate yields (Table 3).

This result outlines here a reversed preference of the silylium attack for the ester function that reveals the structural consequences of the existence of an endocyclic double bond in the 5-membered ring on chemoselectivity as a consequence of the electron density transfer operating from the amide function towards the ester one.

Scheme 4 Synthesis of methyl 1-substituted-5-oxo-4,5-dihydro-1H-pyrrole-3-carboxylate 4a-c and 3,4-cis-disubstituted pyrrolidin-2-one 7.

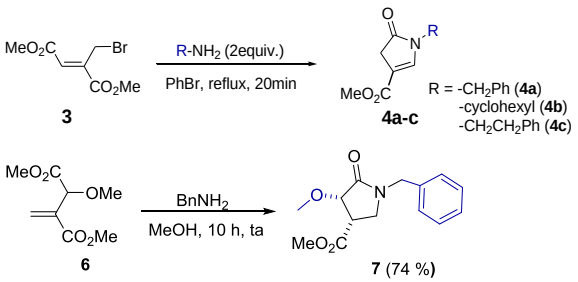

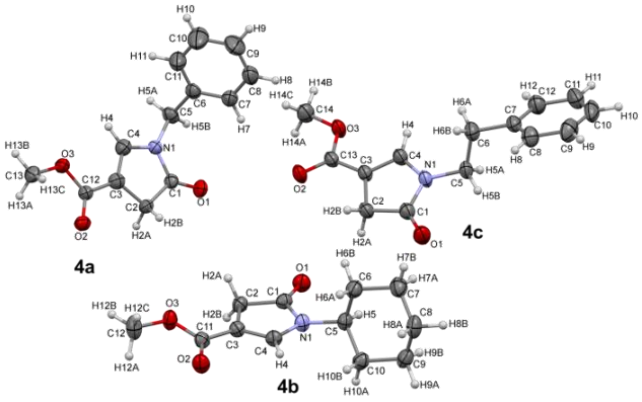

Figure 3. ORTEP drawings of the structures of **4a-c** with atom numbering. The ellipsoids are drawn at 50% probability. See the Suppl. Mat. for further information.

Table 3. Catalytic isomerization of 4a-c with iridium catalyst and Et_3SiH[a,b]

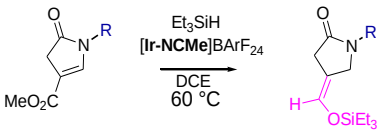

R = -CH_2Ph (**a**), cyclohexyl (**b**), -CH_2CH_2Ph (**c**)

entry	substrate	Et_3SiH (equiv.)	time (h)	product	yield [b] (%)
1	**4a**	8	9	**5a**	45
2	**4b**	5	6	**5b**	40
3	**4c**	6	7	**5c**	39

[a] Reaction conditions: 30 mg (1 equiv.) of **4a-c,** 5 mol% of Ir catalyst and *x* (equiv.) of Et_3SiH in 3 mL of DCE under an argon atmosphere. [b] Isolated yields after purification using flash column chromatography.

Further probe of chemoselectivity on a methoxy-substituted pyrrolidin-2-one. One of the substrates chosen for these preliminary studies was methyl *rac-cis*-1-benzyl-4-methoxy-5-oxopyrrolidine-3-carboxylate **7**, which was readily prepared by a literature method[18] involving conjugate addition of 1 equiv. of benzylamine to the allyl ether **6** in methanol at room temperature and air atmosphere, followed by 5 exo-trig

heterocyclization of the γ-aminoester intermediate, which afforded the 3,4-difunctionalized pyrrolidin-2-one **7** in 74% yield (scheme 4).

Scheme 5 Catalytic reduction of 3,4-disubstituted pyrrolidin-2-one 7 with catalyst and Et_3SiH

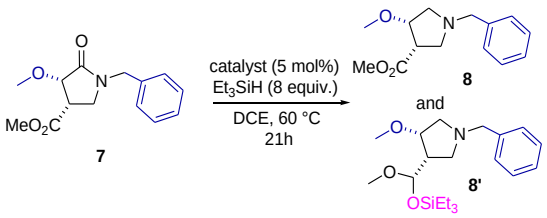

In the presence of Et_3SiH, the iridium catalyst (5 mol%) initiates the catalytic reduction under the same conditions used before. The reaction resulted into the full conversion of **7** by reduction of the amide function alongside the uncontrolled further hydrosilylation of the ester function: a mixture containing **8**, *i.e.* the product of amide reduction yield and **8'**, *i.e.* the product of its partial hydrosilylation, was obtained in 38% and 62% yield respectively (scheme 5).

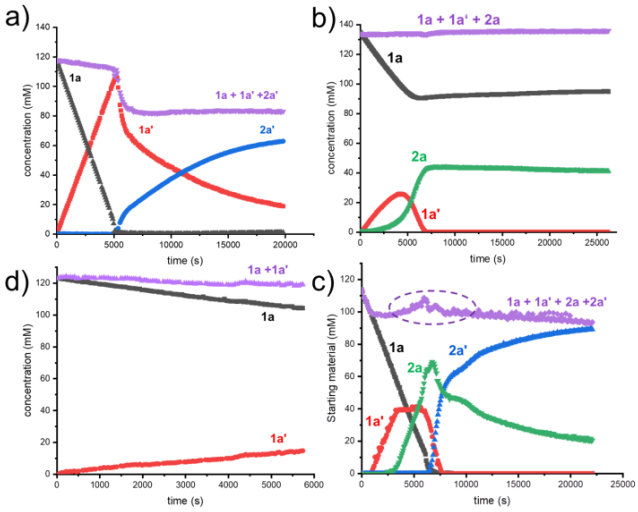

Figure 4. Plots of concentration (mM) of reactants *vs*. time (s) as analyzed with MestRe Nova[19] from the ^{1}H NMR spectroscopic monitoring of the catalyzed reduction (2 mol% of Ir(III) catalyst) of **1a** by Et_3SiH in different solvents, in a spinning argon-sealed J-Young NMR sample tube at 25°C. The top (purple) curves are the control concentration checksums probing the accuracy of the determination of the medium's composition. a) CD_2Cl_2, **1a** ($c_{initial}$= 118 mM), Et_3SiH ($c_{initial}$= 659 mM). b) CD_2Cl_2, **1a** ($c_{initial}$= 135 mM), Et_3SiH ($c_{initial}$= 97 mM). c) ClD_2C-CD_2Cl, **1a** ($c_{initial}$= 114 mM), Et_3SiH ($c_{initial}$= 693 mM). d) d_8.THF, **1a** ($c_{initial}$= 122 mM), Et_3SiH ($c_{initial}$= 764 mM).

^{1}H NMR monitoring of the catalyzed reduction of 1a by Et_3SiH. ^{1}H NMR spectroscopy is particularly well suited for the monitoring of reactions and the observation of reaction transients and intermediates in the making.[20]

The catalytic conversion of **1a** into **2a** was monitored by ^{1}H NMR spectroscopy under different conditions having two goals in scope. The first one was to attempt the observation of key reaction intermediates such as **1a'**, *i.e.* the one resulting from the primary hydrosilylation reaction at the cyclic amide. The second was to gain knowledge of the internal kinetics governing the reduction of **1a**.

The experiments were carried out in CD_2Cl_2, ClD_2C-CD_2Cl and THF-d_8 in sealed J-Young tubes all prepared under a dry Ar gas atmosphere. Reactive solutions were frozen as they were layered in the bottom of the tube before being introduced inside the NMR spectrometer's probe. They were warmed within the NMR probe at 25°C to melt the frozen solutions, mix them by spinning the sealed sample tube and thus trigger the reaction. Acquisition of fast induction decays was started within a few minutes, *i.e.* as soon as satisfactory homogeneity of the field was achieved. Whenever achievable, reaction intermediates were analytically characterized (cf. Suppl. Mat.) from the raw reaction mixture.

The ^{1}H-NMR monitored catalytic runs were carried out under similar conditions of concentration of substrate and catalyst (Figure 4). Notwithstanding the amount of hydrosilane used, all experiments allowed the observation of the formation of a ca. 1:2.5 mixture of diastereomers **1a'**, that is the first intermediates arising from the hydrosilylation of the amide function that precedes the reduction of the cyclic amide into the cyclic amine by the silylium-assisted displacement of the triethylsilyloxy leaving group by the formal hydrido ligand (scheme 3).

The mixture of diasteromers **1a'** is short-lived in the CD_2Cl_2 and ClD_2C-CD_2Cl solutions and is slowly consumed to produce **2a** and **2a'**. In THF-d_8, **1a'** is the only product of the reaction of **1a** with a *ca.* 6-fold excess of Et_3SiH and any further evolution of the reaction seems inhibited putatively by the capture of the silylium by THF.

The kinetic profile of the consumption of **1a** and of the formation of **1a'** in the two chlorinated solvent in the presence of a *ca*. 6-fold excess of Et_3SiH matches (pseudo) zero-order reaction kinetics with a rate constant k^0 of $(2.15 \pm 0.04)10^{-2}$ M s^{-1} in CD_2Cl_2 (Figure 4a) and $(1.6_5 \pm 0.1)10^{-2}$ M s^{-1} in ClD_2C-CD_2Cl (Figure 4c).

In both chlorinated solvents the full consumption of **1a** was achieved in less than 2h. Note that the control concentration checksum curve (upper purple curves in Figure 4), used here to verify the conservation of matter over time with **1a** and its structural derivatives, reveals that significant signal integration inconsistencies are produced by the overlap of signals in CD_2Cl_2 (Figure 4a), which prevents the localization and precise quantification of **2a** from NMR spectra.

In other terms, it remains plausible that like in Figure 4c, compound **2a** may appear for a short time in the medium and be consumed to give **2a'**.

Given the conditions of the reaction carried out here in a sealed tube the observed conversion of **2a** into **2a'** (Figure 4c) seemingly results from the strictly anhydrous and anaerobic conditions achieved within the J-Young tube, which supposedly minimize the interference of adventitious moisture with highly electrophilic silylium species as compared to the standard Schlenk setup used in our catalytic runs. This is evidenced clearly in Figure 4b which was carried out in quasi stoichiometric conditions between **1a** and Et_3SiH. The plot shows the sensible emergence of **1a'** in the early stages of the

reaction with its maximum concentration reaching *ca*. 30 mM nearly at 5000 s before receding at *t*~ 6500 s to **2a**, which reaches an optimal concentration of *ca*. 45 mM at *t*~ 7000 s.

Scheme 6. Proposed rationale for the pseudo first order rate inferred from ^{1}H NMR-monitored kinetic studies based on the saturation of the catalyst in a Michaelis-Menten mechanism. The *aa* index in [1a-SiEt$_3$•IrH]$_{aa}^+$ stands for silylium activated amide undergoing hydrido ligand binding at the amide's carbonyl C atom.

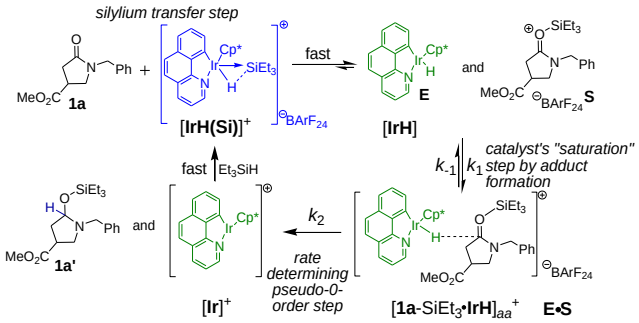

Michaelis-Menten substrate saturation regime

$d[\mathbf{1a'}]/dt \sim [(k_1k_2[\mathbf{S}])/(k_{-1} + k_2)][\mathbf{E}]_0$

fast production of **S** $\Rightarrow$ [**S**] not a limiting factor $\Rightarrow$pseudo zero-order rate law

[**1a**] >>[**E**]$_0$

Worthy to note, the pseudo zero-order rate of the formation of **1a'** resembles that of a Michaelis-Menten mechanism[21] (abbr. 3M) in the so-called "substrate saturation regime"[22] where the hydrido-iridium(III) catalyst [**IrH**], referred to as **E** in scheme 6 according to the accepted notation for the 3M, would give rise to the reactant complex [**1a**-SiEt$_3$•[**IrH**]]$^+$ (also referred to as the [**E•S**] adduct in scheme 6) resulting from a carbon-hydrido ligand interaction between the transient [**1a**•SiEt$_3$]$^+$ adduct referred to as **S** in scheme 6 (vide infra) and [**IrH**]. The saturation regime entails that the formation of the Ir-silane adduct *in situ* (scheme 3) should not limit the availability of the [**1a**•SiEt$_3$]$^+$ adduct in the medium (referred to as **S** in scheme 6) and is way faster than the formation of the [**1a-SiEt$_3$•IrH**]$_{aa}^+$ adduct (cf. [**E•S**] adduct, scheme 6). This would indeed explain the total selectivity of the first step of the process for the hydrosilylation of the cyclic amide function by suggesting consequently that the amide has a much stronger affinity for the [SiEt$_3$]$^+$ species than the competing ester function. This assumption would also entail that the rate determining state in the formation of **1a'** is the hydrido ligand transfer in the [**1a**-SiEt$_3$•**IrH**]$_{aa}^+$ adduct from the Ir center to the carbonyl's carbon (*cf.* [**E•S**], scheme 3). Figures 4a-c give also access to initial rates of formation of **2a** and **2a'**, which seemingly follow a pseudo-first order rate laws.

Given the large inconsistency in the control concentration checksum curve in Figure 4a, Figure 4c was used instead to extract more reliable initial formation rate constants of **2a** and **2a'**, which amount $k_i^1(\mathbf{2a})$= (1.8 ± 0.05)10^{-2} M s^{-1} and $k_i^1(\mathbf{2a'})$= (5.1 ± 0.1)10^{-2} M s^{-1} respectively. These values demonstrate that in the presence of a large excess of Et$_3$SiH in a strictly anhydrous medium the hydrosilylation of the ester function of **2a** is unavoidable once the amide has underwent complete reduction.

Table 4. Values of V_{min} electrostatic potentials at the O atoms of the ester and amide functions of 1a and 4a and computed reaction enthalpies and Gibbs free energy of the formation of adducts [1a/4a-SiEt$_3$]$_{a/e}^+$ by the capture of the [Et$_3$Si]$^+$ moiety from the [IrH(Si)]$^+$ species by either amide or ester functional groups.

substrate	$V_{min}(O_{ester})/(O_{amide})$ (eV)	capturing function	adduct	ΔH, ΔG (kcal/mol)
1a	-1.28/-1.72	amide@**1a**	[1a-SiEt$_3$]$_a^+$	-1.8, -1.5
		ester@**1a**	[1a-SiEt$_3$]$_e^+$	+10.9, +11.8
4a	-1.47/-1.43	amide@**4a**	[4a-SiEt$_3$]$_a^+$	+15.2, +14.8
		ester@**4a**	[4a-SiEt$_3$]$_e^+$	+12.1, +12.6

Calculations were carried out at the COSMO(DCE)/PBE-D4(EEQ)/all electron TZP level. In [**1a/4a**-SiEt$_3$]$_{a/e}^+$ the *a* index corresponds to the silylium binding the amide, while the *e* index relates to ester binding.

Theoretical insight into the chemoselectivity of the catalytic reduction of 1a and 4a. The question of the chemoselectivity can theoretically be addressed from several viewpoints. The first one may consider chemoselectivity as being partly predetermined by the electronic properties of the substrate. The second one may consider that the origin of chemoselectivity might lie also in the rate determining states.

As a matter of fact, the reduction reaction based on the catalytic activation of Et$_3$SiH is governed by the affinity of the substrate for the triethylsilylium [Et$_3$Si]$^+$, which determines the function that will subsequently undergo hydride transfer from [**IrH**]. The electrostatic control of the activation of substrates by a silylium can readily be approached quite intuitively by weighing the minima of the electrostatic potential V_{min}, corresponding to the most likely Lewis basic sites for an interaction with [Et$_3$Si]$^+$.Two prototypical cases were chosen here, that is namely **1a** and **4a**, which display rather different reactivity in the reduction reaction. The computation of the minimum electrostatic potentials V_{min} at the key O atoms of the ester and of the cyclic amide reveals a differentiation between **1a** and **4a**, which, in spite of a minor structural difference, i.e. the intracyclic unsaturation, display an opposite behavior in the catalysis; the amide function being favored for the reduction reaction in the former case, while the ester is selectively attacked in the latter substrate. Table 4 shows indeed that **1a** bears a stronger (more negative) charge density V_{min} at the O atom of the amide while the situation is slightly reversed in **4a** with the ester dominating slightly over the amide, the N atom of which is seemingly engaged in conjugation with the ester function.

This coulombic control translates into distinct values of affinities of each functional group for the [Et$_3$Si]$^+$ (Table 4 and Figure 5). When modelled by considering the transfer from the Ir-hydrosilane adduct [**IrH(Si)**]$^+$ to **1a**, the enthalpy is slightly exothermic only for the capture of [Et$_3$Si]$^+$ by the amide's carbonyl oxygen atom, while the capture by the ester is largely endothermic by over 10 kcal/mol.

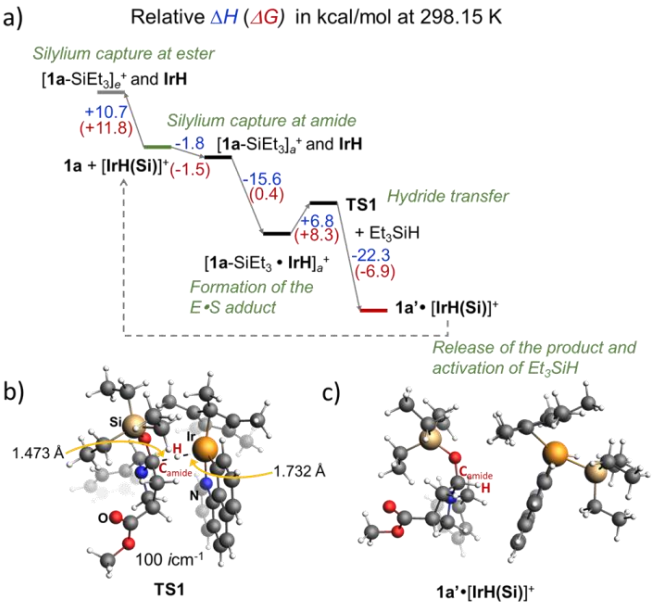

Figure 5. a) Energy profile of the first reduction of **1a** occurring at the amide function. b) singlet-transition state geometry for the hydride transfer from the hydrido-iridium fragment to the triethylsilylium adduct of **1a**. c) singlet-state van der Waals adduct resulting from the reduction of the [**1a**-$SiEt_3$]$^+$ adduct and the reactivation of the released iridacycle by reaction with Et_3SiH.

In the case of **4a**, both captures of the triethylsilylium moiety by the amide and the ester functions are endergonic, but this endergonicity is by 2 kcal/mol less pronounced for the ester function (Table 4, Figure 5), which might serve as a basis for rationalizing the reversed selectivity of the catalyzed reaction of **4a** with Et_3SiH that first targets the $\alpha\beta$-unsaturated ester function.

Figure 5a illustrates for **1a** the higher affinity for [Et_3Si]$^+$ of the amide function, the silylium's capture being slightly exergonic while the capture by the ester is way endergonic by more than +12 kcal/mol. Exploration of the energy profile (Figure 5a) of the reduction of **1a** reveals also that the Michaelis-Menten assumption of a saturation of the iridium catalyst by the substrate being at the origins of the pseudo zero-order kinetics of formation of intermediate **1a'** is based: figure a5 shows that the interaction of [**IrH**] with [**1a**-$SiEt_3$]$_a^+$ is strongly exothermic (ΔH ~ -22 kcal/mol).

In other previously reported cases implying the same type of iridacyclic catalyst such catalyst-substrate adducts escaped DFT localization of the potential surface and were not isolated as local mimima: rather, the hydrido ligand transfer used to occur in an apparent "barrier-less" fashion.[14a,14b,15]

In the present study, such reactant complexes were sought computationally and successfully isolated on the potential surface in the case of [**1a**-$SiEt_3$]$_a^+$ (Figure 5) and for [**4a**-$SiEt_3$]$_{a,e}^+$ (Figure 6) for the first reduction reaction step. Two possible [**4a**-$SiEt_3$]$^+$ adducts were considered (amide and ester activation by [$SiEt_3$]$^+$) with three potential interactions with the hydrido ligand of [**IrH**], i.e. namely: the interactions with amide's C atom [**4a**-$SiEt_3$•**IrH**]$_{aa}^+$, ester's C atom [**4a**-$SiEt_3$•**IrH**]$_{ee}^+$ and ethylenic C atom connected to the nitrogen atom [**4a**-$SiEt_3$•**IrH**]$_{ec}^+$ (Figure 6).

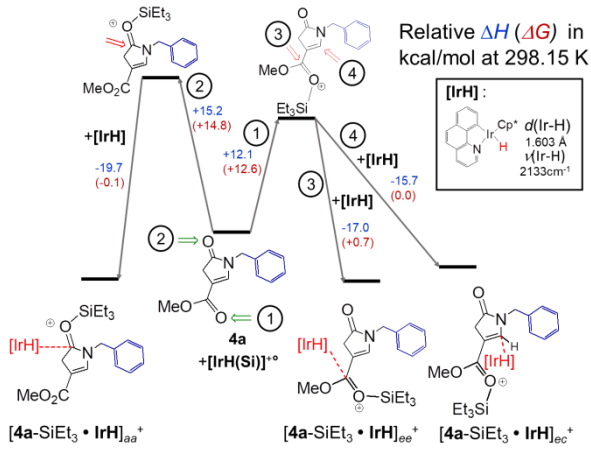

Figure 6. Thermochemistry of the capture of the [Et_3Si]$^+$ moiety from the [**IrH(Si)**]$^+$ adduct by either amide or ester functions of **4a** and the formation of reactant complexes by association of the cationic [**4a**-$SiEt_3$]$^+$ and the hydrido-iridium(III) intermediate [**IrH**], that is [**4a**-$SiEt_3$•**IrH**]$_{aa,ee \text{ and } ec}^+$ where the indexes mean as follows: *aa* for silylium bound to the amide's carbonyl the hydrido ligand interacting with the carbonyl's carbon, *ee* for silylium bound to the ester's carbonyl the hydrido ligand pointing at ester's carbonyl carbon, *ec* for silylium bound to the ester's carbonyl while the hydrido ligand interacts with the β ethylenic carbon.

Theoretical investigation of the activated substrate-hydridoiridium adducts. Compared to [**IrH**], the computed Ir-H bond stretching vibrational band of the adducts [**1a**-$SiEt_3$•**IrH**]$_{aa \text{ and } ee}^+$ and [**4a**-$SiEt_3$•**IrH**]$_{aa,ee \text{ and } ec}^+$ show significant variations of the computed vibrational frequency $\Delta\nu$ with -29 cm^{-1} < $\Delta\nu$ < +64 cm^{-1}. These variations could suggest a vibrational Stark effect[23], in the event the [IrH] moiety would not be bonded covalently to the activated substrate. Indeed, it could suggest that the local electric field influences the polarization of the Ir-H bond in the [**IrH**] species, thus affecting presumably its propensity to transfer the hydrido ligand. In fact, this assumption might only be true in the early stages of the formation of the considered [**1a**/**4a**-$SiEt_3$•**IrH**]$^+$ adducts. The analysis of the inter-fragment interaction in the latter adducts leads to a different interpretation of the stretching Ir-H frequency shift : it is caused by the nature of the donor-acceptor interaction of weak but significant covalent character between the bridging hydrido ligand of the metallacycle and the cationic organic substrate. To understand the electronic properties of the [**1a**/**4a**-$SiEt_3$•**IrH**]$^+$ adducts several bond analysis tools were used that provided complementary descriptions of the interplay of covalence and noncovalence.

Table 5. Analysis of the interaction of the hydrido-iridium [IrH] species with adducts [1a-SiEt$_3$]$^+$ and [4a-SiEt$_3$]$^+$ by IQA and ETS-NOCV.

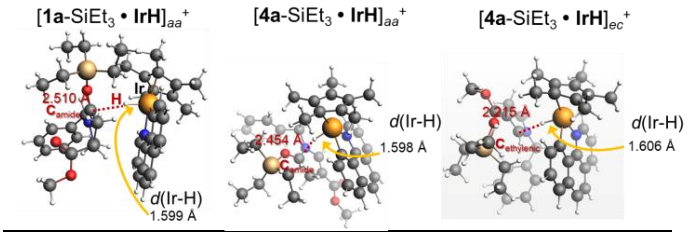

	[**IrH**]	[**1a**-SiEt$_3$•**IrH**]$_{aa}^+$	[**4a**-SiEt$_3$•**IrH**]$_{aa}^+$	[**4a**-SiEt$_3$•**IrH**]$_{ec}^+$
IQA analysis[a](V in kcal/mol)				
Ir-H				
V_{int}	-130.9	-126.1	-126.8	-119.9
$V_{cov.}$(%)	-129.4(98.8)	-125.6(99.6)	-125.0(98.6)	-122.0 (101.8)
V_{ionic}(%)	-1.5(1.1)	-0.5 (0.4)	-1.8 (1.4)	+2.1 (-1.8)
H-C	-			
V_{int}	-	-31.8	-34.5	-20.4
$V_{cov.}$ (%)	-	-3.0 (9.4)	-3.7(10.7)	-12.8 (62.7)
V_{ionic}(%)	-	-28.8 (90.6)	-30.8 (89.3)	-7.6 (37.3)
ETS-NOCV[b]$_t$(E in kcal/mol)				
ΔE_{in}	-	-61.1	-67.4	-69.7
ΔE_{orb}		-11.3	-12.0	-13.9
ΔE_k		-1.8	-2.2	-5.5
atomic Bader charges q and intra-fragment charge variations Δq [a]				
q(Ir)	+0.614	+0.598	+0.611	+0.602
q(H)	-0.187	-0.167	-0.176	-0.140
q(C)	-	+1.206	+1.203	+0.409
Δq([**IrH**])	0	+0.08	+0.09$_5$	+0.16
IGM-Independent Bond Strength Index[c]				
Ir-H	0.427	0.429	0.432	0.432
H-C	-	0.026	0.029	0.057
distances[b](in Å)				
d(Ir-H)	1.603	1.599	1.598	1.606
d(H-C)	-	2.510	2.454	2.215
computed Ir-H stretching mode[b] (reciprocal wavelengths in cm^{-1})				
ν(Ir-H)	2133	2186	2200	2104

[a] carried out at the PBE-D4(EEQ)/TZ2P level/ COSMO(DCE). [b] carried out at the ZORA-PBE-D4(EEQ)/all electron TZP level/COSMO(DCE). [c] computed at the PBE-D3(BJ)/ZORA-def2-TZVP & SARC-ZORA-TZVP for Ir /SDM(DCE)

Hence, Table 5 lists the main features of the optimized singlet ground state local minima of those adducts by gathering the Interacting Quantum Atoms[24] (IQA) and Independent Gradient Model (IGM)/Intrinsic Bond Strength Index (IBSI) analyses[25] of key bonds, the Extended Transition State – Natural Orbitals for Chemical Valence[26] (ETS-NOCV) analysis of the orbital interaction between the two considered fragments and the local Bader charges[27] deduced from the Quantum Theory of Atoms in Molecule (QTAIM-charges).

Δq([**IrH**]) (Table 5) is the variation of the sum of QTAIM-charges at the [**IrH**] moiety upon interaction with [**1a**/**4a**-SiEt$_3$]$^+$ and materializes the extent of charge density transfer from the [**IrH**] species to the activated susbtrate. The largest charge transfer is observed for [**4a**-SiEt$_3$•**IrH**]$_{ec}^+$, which is not unexpected given that this adduct is the one with the shortest H-C distance and the highest covalent character for the H-C interaction like revealed by the IQA analysis.

The IQA energy partitioning method[24a,28] is based on real-space partitioning of the molecular space; this method, when extended to the Kohn-Sham DFT framework, gives access to a semi-quantitative partitioning of energy contributions of exchange-correlation and of coulombic interaction terms for two-atom interactions within a molecule. The interatomic interaction energy V_{int}^{AB} is the sum of a covalent V_{cov}^{AB} and an ionic contribution V_{ionic}^{AB}: $V_{int}^{AB} = V_{ionic}^{AB} + V_{cov}^{AB}$ (Table 5). These interatomic energies weigh the covalent and coulombic contributions and allow to firmly establish which character is dominant.

IQA analyses of [**1a**-SiEt$_3$•**IrH**]$_{aa}^+$ and [**4a**-SiEt$_3$•**IrH**]$_{aa}^+$ show that the hydrido ligand attractively interacts with the triethylsilyl-activated substrate with the carbon atom where it will be transferred by dominating coulombic (ionic) interactions, the contribution of which represents about 90% of the interatomic interaction potential V_{int}. Only in the case of [**4a**-SiEt$_3$•**IrH**]$_{ec}^+$ the covalent contribution predominates in the V_{int} value.

The three cases treated here cannot be directly compared though due to the large difference of hydrido-to-carbon distances that span 2.510 ([**1a**-SiEt$_3$•**IrH**]$_{aa}^+$) to 2.215 Å ([**4a**-SiEt$_3$•**IrH**]$_{ec}^+$) (Table 5). Nonetheless, the ETS-NOCV analysis[26] that provides a detailed breakdown of orbital interactions between the [**IrH**] and the silylated substrates, which details the covalent contributions weighed by IQA. This interacting fragment-based analysis indicates that the Ir-H…C interaction has a low ΔE_k orbital interaction energy value in all cases, the highest value of -5.5 kcal/mol being for [**4a**-SiEt$_3$•**IrH**]$_{ec}^+$ for the interaction of the hydrido ligand with the N-bound intracyclic ethylenic carbon. This interaction is largely dominated by a covalent character according to the IQA analysis (Table 5) and matches what is often assigned to an orbital-controlled pathway, while other interactions that are dominated by coulombic interactions would rather match a charge-controlled pathway.

The NCI-Plot analysis[29] (Figure 7a) reveals local repulsive, non-bonding van der Waals contacts and attractive noncovalent interactions by means of signed reduced density gradient isosurfaces, which have been shown to be systematically encountered[30] in key reactant complexes of base-assisted C-H bond metalation mechanism[31] and in reductive elimination reactions.[32] Here the NCI-Plot graph shows a typical attractive lenticular domain between the hydrido ligand and the carbon atom subjected to reduction in the case of [**4a**-SiEt$_3$•**IrH**]$_{ec}^+$. In all other cases where the hydrido-to-carbon distance is longer no attractive NCI domain in the H-C segment is noted but rather a non-bonding one is observed.

The IGM-δg^{inter} descriptor is a measure of the electron sharing caused by the electron density interference between two user-defined fragments.[25a,25b] It assesses the mutual density penetration by the deviation of the true electron density gradient from a non-interacting reference, i.e. the independent gradient model bearing the same electron density as the real system.

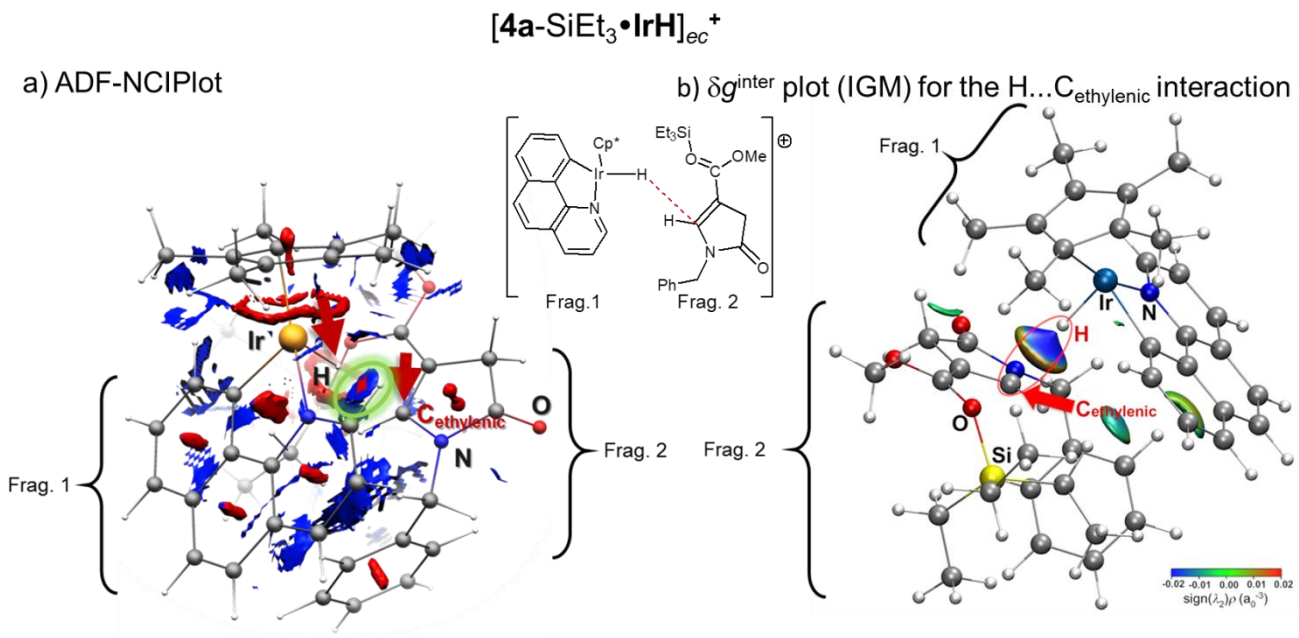

Figure 7. ADF-NCIPlot and IGMPlot analyses for [**4a**-SiEt$_3$•**IrH**]$_{ec}^+$: (a) full ADF-NCIplot (cutoff values : s=0.5, ρ= 0.02 a_0^{-3}) showing the typical lenticular attractive isosurface (circled with a green aura) between the hydridic H and the ethylenic C (noncovalent interactions are materialized by the reduced density gradient isosurface coloured according to the signed density: red for attractive domains, and blue for repulsive or non-bonding domains), the Si centre is in the dimmed back ; (b) IGM-δg^{inter} isosurface plot for the interaction between fragments (cutoff: δg^{inter} = 0.01 a_0^{-4}, and blue-green-red colour code in the range -0.02 < sign(λ_2)ρ < 0.02 a_0^{-3}) of the interaction between the [**IrH**] species (fragment 1) and the [**4a**-SiEt$_3$]$_e^+$ adduct (fragment 2) in the [**4a**-SiEt$_3$•**IrH**]$_{ec}^+$ system showing the lenticular attractive isosurface (circled in red) between the hydridic iridium-bound H and the ethylenic C (noncovalent interactions are here materialized by the independent gradient isosurface coloured according to the signed density from blue = attractive interactions to red = repulsive interactions).

Like many QTAIM-based methods[27] the IBSIs are not impacted by basis set superposition errors (BSSE) and therefore they allow a "reputation-based" characterization of atom-pair interactions steming from Hénon's correlation of IBSI values with notorious types of atom pair interactions taken from a vast variety of reference compounds. [25c] Atom-pair interactions are thus categorized as noncovalent (0 a_0^{-1}< IBSI < 0.15 a_0^{-1}), coordination (0.15 a_0^{-1} < IBSI < 0.6 a_0^{-1}) or covalent (IBSI > 0.15 a_0^{-1}) according to reference standards. [25c] The IGM-IBSI descriptor[25,33] is a measure of the electron sharing caused by the electron density interference between two user-defined fragments. It assesses accurately the mutual density penetration by the deviation of the true electron density gradient from a non-interacting reference, *i.e.* the independent gradient model bearing the same electron density as the real system. Plotting the IGM-δg^{inter} isosurface (Figure 7b) in the real space allows the visualization of noncovalent interaction domains in a more discriminating fashion than NCIPlot like shown in Figure 7b. As for the NCI-Plot, the IGM-δg^{inter} isosurface shows a typical attractive lenticular domain between the hydrido ligand and the carbon atom subjected to hydride attack in the case of [**4a**-SiEt$_3$•**IrH**]$_{ec}^+$.

Here the IBSI of the Ir-H bond, *i.e.* ~ 0.43 (Figure 7b), matches the values for coordination bonds[25c] and does not change drastically upon interaction with either [**1a**-SiEt$_3$]$^+$ or [**4a**-SiEt$_3$]$^+$**.** In turn the IBSI value of the hydrido-to-susbtrate's carbon interaction is clearly different depending of the nature of the function facing the hydrido ligand, varying by almost a factor of 2 from 0.026 and 0.029 to 0.057 for [**1a**-SiEt$_3$•**IrH**]$_{aa}^+$, [**4a**-SiEt$_3$•**IrH**]$_{aa}^+$ and [**4a**-SiEt$_3$•**IrH**]$_{ec}^+$ respectively. The increase of the IBSI as the interatomic distance shortens is consistent with an increased charge transfer. In the context of the competition that is expected between [**4a**-SiEt$_3$•**IrH**]$_{aa}^+$ and [**4a**-SiEt$_3$•**IrH**]$_{ec}^+$ this difference of IBSI rationalizes the preference given to the reductive double bond isomerization reaction, which requires a first step of hydride attack at the ethylenic position.

CONCLUSION

This study demonstrates that the performance of the benzo[*h*]quinoline-based acetonitriloiridacycle in the catalyzed reduction and hydrosilylation of multifunctional organic substrates such as the γ-lactams addressed here depends essentially on the selectivity of the capture of the transient silylium species released in the medium by the various functions present in the substrate. The outcome of the catalysis is, in a second stage, also determined by the ability of the hydrido-iridium intermediate to transfer the hydrido ligand to the substrate, a process that is either charge or orbital-controlled depending on the organic function facing the hydrido ligand in the key reactant complex. Kinetic studies carried out with **1a** as a substrate show that the first step of the reduction of the intra-cyclic amide function is the formation of the product of hydrosilylation of amide's carbonyl, that is a *N*-substituted silyl ether produced by a pseudo-zero-order rate law that

matches a Michaelis-Menten catalysis under the catalyst's saturation regime. In all the cases treated here, the productiveness of the catalyzed reduction by Et_3SiH is remarkable and confirms the potential of the used benzo[*h*]quinoline-derived cationic iridacyclic catalyst.[14b,15] On the issue of selectivity of the reductive reactions, the main conclusions drawn are the following: 1) the catalysis is mostly governed by the silylium's reactivity, that is chemioselectivity is driven by substrate's site affinity for silylium, 2) the transfer of hydride to the silylium-activated substrate is not necessarily charge controlled, 3) substitution of the amide's intra-cyclic N centre with an ethylenic moiety reduces the charge density at the amide carbonyl oxygen centre which results in a significant decrease of the affinity for the silylium cation and overall chemioselectivity, 4) a protic function such as hydroxy in **1k** is readily silylated without compromising the main amide's reduction and finally, 5) even though their affinity for the silylium transient might be significant, catalytic runs showed that methoxy and dioxomethylene groups (in **2c**, **2e** and **2d** and in **7**) are left untouched. Further investigation are underway to attempt the capture of the spectroscopic signature of the key [**1a**/**4a**-$SiEt_3$•**IrH**]$^+$ adducts.

EXPERIMENTAL SECTION

General Considerations: All reagents were purchased from commercial suppliers and used without further purification. Anhydrous 1,2-dichloroethane and dichloromethane were distilled under an argon atmosphere from CaH_2 prior to use. Tetrahydrofuran was distilled under an argon atmosphere from sodium benzophenone prior to use. Reactions requiring anhydrous conditions were carried out using Schlenk techniques under argon atmosphere. Deuterated halogenated solvents for NMR use were all degassed by the freeze-pump-thaw procedure and dried by stirring a suspension of fresh CaH_2 overnight under argon. The resulting suspension was subsequently filtered through dry Celite^{TM} and stored under argon over dry molecular sieves in a Schlenk tube. Thin layer chromatography was performed using silica gel plates (60 F_{254}); visualization was achieved by UV lamp or upon revelation with $KMnO_4$ solution. Flash chromatography was performed on silica gel (Aldrich 40-63 μm). NMR spectra were recorded on Bruker NMR spectrometers (DPX 400, Avance NEO and III HD 500) at room temperature. ^{1}H NMR (500), ^{13}C NMR (126), ^{29}Si NMR (99.37) chemical shifts (expressed in parts per million) were recorded in $CDCl_3$ or CD_2Cl_2 in most cases unless otherwise stated and referenced to residual solvent peaks (with $CDCl_3$ at 7.26 ppm for ^{1}H and 77.16 ppm for ^{13}C, with CD_2Cl_2 at 5.32 and 53.84 ppm for ^{13}C). ^{1}H NMR data are reported as follows: chemical shift (ppm, scale), multiplicity, coupling constant (Hz) and integration. The abbreviations used for NMR signal multiplets stands as: *s*, singlet; *d*, doublet; *dd*, doublet of doublet; *ddd*, doublet of doublet of doublet, *dq*, doublet of quartet; *t*, triplet; *q*, quartet; *quint*, quintet; *m*, multiplet. Data for ^{13}C NMR are reported in chemical shift (ppm). Infrared spectra were recorded using Bruker FT-IR spectrometer. High-resolution mass spectra were obtained by ESI on a TOF mass analyzer. Elemental analyses were achieved with Thermo Scientific FLASH 2000 CHNS/O analyzers. Single crystal X-ray diffraction data collection was carried out on a Bruker APEX II DUO Kappa-CCD and Bruker PHOTON III diffractometer. The catalyst used in this study, *i.e.* [acetonitrilo,(η^5-pentamethylcyclopentadienyl)(benzo[*h*]quinolinyl,$\kappa C_{10},N$)iridium][tetrakis(3,5-bis(trifluoromethyl)phenyl)borate] was synthesized according to a reported procedure.[14b,15]

General procedure for the synthesis of pyrrolidin-2-one 1
Pyrrolidin-2-ones **1** were prepared according to a literature procedure[17c,34] with minor modifications. 1.1 equivalent of appropriate primary amine (3.4 mmol) was added dropwise to a solution of dimethyl itaconate (3.1 mmol, 500 mg, 1 equiv.) in methanol (~5 mL), the reaction mixture was stirred at room temperature and monitored by TLC. At the end of the reaction the solvent was removed under vacuum and the crude product was purified by silica gel chromatography eluting with a mixture of *n*-pentane and ethyl acetate to afford desired pyrrolidin-2-ones. When the amine was tyramine, the crude product was purified by recrystallisation using a mixture of hexane/diethyl ether (7/3). Product **1a-c**, **1g** and **1k** are known compounds.[17c,34]

Methyl-1-benzyl-5-oxopyrrolidine-3-carboxylate **1a.**[17c,34a] Following general procedure **A** the title product was purified by flash chromatography (*n*-pentane / EtOAc = 4:6) yielding lactam **1a** (630 mg, 85%) as colorless oil which solidified on standing. Anal. calcd for $C_{13}H_{15}NO_3$: C, 66.94; H, 6.48; N, 6.00. Found: C, 66.95; H, 6.50; N, 6.02. IR, ν_{max}/cm^{-1} (neat): 1733 (C(O)O), 1689 (C(O)N). ^{1}H NMR (500 MHz, $CDCl_3$): δ 7.35-7.22 (m, *aromatic* 5H), 4.46 (AB, J = 15.0 Hz, 2H), 3.70 (s, 3H), 3.50-3.43 (m, 2H), 3.24-2.17 (m, 1H), 2.74 (qd, J = 17.2, 8.7 Hz, 2H). ^{13}C{^{1}H} NMR (126 MHz, $CDCl_3$): δ 173.3 (*C*ON), 172.3 (*C*OO), 135.9 (*aromatic =C*), 128.8 (*aromatic* 2 (=*C*H), 128.2 (*aromatic* 2 (=*C*H), 127.8 (*aromatic =C*H), 52.5 (O*C*H$_3$), 48.6 (*C*H$_2$Ph), 46.7 (*C*H$_2$N), 36.0 (*C*H$_2$CO), 34.2 (*C*HCO). HRMS (ESI) calcd for $C_{13}H_{16}NO_3$ $[M+H]^+$ 334.1130. Found 334.1115.

Methyl-1-(4-chlorobenzyl)-5-oxopyrrolidine-3-carboxylate **1b**[34b]. Following the general procedure A the title product was purified by flash chromatography (*n*-pentane / EtOAc = 4:6) yielding lactam **1b** (550 mg, 65%) as colorless oil which solidified on standing. Anal. calcd for $C_{13}H_{14}ClNO_3$: C, 58.33; H, 5.27; N, 5.23. Found: C, 58.13; H, 5.22; N, 5.40. IR, ν_{max} /cm^{-1} (neat): 1731 (COO), 1675 CON). ^{1}H NMR (500 MHz, $CDCl_3$) δ 7.27 (d, J = 7.8 Hz, *aromatic* 2H), 7.14 (d, J = 7.7 Hz, *aromatic* 2H), 4.39 (s, 2H), 3.67 (s, 3H), 3.46-3.40 (m, 2H), 3.21-2.15 (m, 1H), 2.76-2.65 (m, 2H). ^{13}C{^{1}H} NMR (126 MHz, $CDCl_3$) δ 173.1 (*C*ON), 172.4 (*C*OO), 134.5 (*aromatic =C*), 133.6 (*aromatic =C*-Cl), 129.5 (*aromatic* 2 (=*C*H)), 128.9 (*aromatic* 2 (=*C*H)), 52.5 (O*C*H$_3$), 48.4 (*C*H$_2$Ar), 45.9 (*C*H$_2$N), 35.8 (*C*H$_2$CO), 34.0 (*C*HCO). HRMS (ESI) calcd for $C_{13}H_{15}ClNO_3$ $[M+H]^+$ 268.0740. Found 268.0725.

Methyl-1-(4-methoxybenzyl)-5-oxopyrrolidine-3-carboxylate **1c**[17c]. Following the general procedure A the title product was purified by flash chromatography (*n*-pentane / EtOAc = 4:6) yielding lactam **1c** (500 mg, 60%) as colorless oil which solidified on standing. Anal. calcd for $C_{14}H_{17}NO_4$: C, 63.87; H,

6.51; N, 5.32. Found: C, 63.82; H, 6.47; N, 5.28. IR, ν_{max} / cm^{-1} (neat): 1727 (COO), 1671 (CON). ^1H NMR (500 MHz, $CDCl_3$) δ 7.14 (d, *J* = 8.3 Hz, *aromatic* 2H), 7.84 (d, *J* = 8.3 Hz, *aromatic* 2H), 4.37 (AB, *J* = 15.0 Hz, 2H), 3.77 (s, 3H), 3.67 (s, 3H), 3.42 (d, *J* = 7.7 Hz, 2H), 3.20-2.14 (m, 1H), 2.70 (qd, *J* = 17.1, 8.7 Hz, 2H). $^{13}C\{^1H\}$ NMR (126 MHz, $CDCl_3$) δ 173.3 (*C*ON), 172.2 (*C*OO), 159.2 (*aromatic =C*), 129.6 (*aromatic* 2 (=*C*H)), 128.0 (*aromatic =C*), 114.1 (*aromatic* 2 (=*C*H)), 55.3 (O*C*H_3), 52.5 (O*C*H_3), 48.40 (*C*H_2Ar), 45.9 (*C*H_2N), 35.9 (*C*H_2*C*O), 34.0 (*C*HCO). HRMS (ESI) calcd for $C_{14}H_{17}NO_4$ +K $[M+K]^+$ 302.0796. Found 302.0789.

Methyl-1-(piperonyl)-5-oxopyrrolidine-3-carboxylate **1d**. Following general procedure **A** the title product was purified by flash chromatography (*n*-pentane / EtOAc = 4:6) yielding lactam **1d** (790 mg, 90%) as colorless oil, which solidified on standing. Anal. calcd for $C_{14}H_{15}NO_5$: C, 60.64; H, 5.45; N, 5.05. Found: C, 60.65; H, 5.53; N, 5.06. IR, ν_{max} /cm^{-1} (neat): 1729 (COO), 1674 (CON). ^1H NMR (500 MHz, $CDCl_3$) δ 6.74-6.67 (m, *aromatic* 3H), 5.93 (s, 2H), 4.35 (AB, *J* = 14.6 Hz, 2H), 3.69 (s, 3H), 3.45 (d, *J* = 7.4 Hz, 2H), 3.22-3.15 (m, 1H), 2.71 (qd, *J* = 17.2, 8.6 Hz, 2H). $^{13}C\{^1H\}$ NMR (126 MHz, $CDCl_3$) δ 173.2 (*C*ON), 172.3 (*C*OO), 148.1 (*aromatic =C*), 147.3 (*aromatic =C*), 129.8 (*aromatic =C*), 121.7 (*aromatic =C*H), 108.7 (*aromatic =C*H), 108.4 (*aromatic =C*H), 101.2 (O-*C*H_2-*O*), 52.5 (O*C*H_3), 48.4 (*C*H_2Ar), 46.4 (*C*H_2N), 35.9 (*C*H_2CO), 34.1 (*C*HCO). HRMS (ESI) calcd for $C_{14}H_{15}NO_5$ + K $[M+K]^+$ 316.0587. Found 316.0582.

Methyl-1-(2-methoxybenzyl)-5-oxopyrrolidine-3-carboxylate **1e.** Following the general procedure **A** the title product was purified by flash chromatography (*n*-pentane / EtOAc = 3:7) yielding lactam **1e** (600 mg, 72 %) as colourless oil. Anal. calcd for $C_{14}H_{17}NO_4$: C, 63.87; H, 6.51; N, 5.32. Found: C, 63.48; H, 6.48; N, 5.45. IR, ν_{max}/cm^{-1} (neat): 1733 (COO), 1683 (CON). ^1H NMR (500 MHz, $CDCl_3$) δ 7.26 (t, *J* = 10.5 Hz, *aromatic* 1H), 7.19 (d, *J* = 7.5, *aromatic* 1H), 6.91 (t, *J* = 8.5 Hz, *aromatic* 1H), 6.86 (d, *J* = 8.0 Hz, *aromatic* 1H), 4.52-4.46 (m, 2H), 3.82 (s, 3H), 3.70 (s, 3H), 3.49 (d, *J* = 7.5 Hz, 2H), 3.22-3.15 (m, 1H), 2.70 (qd, *J* = 17.1, 8.0 Hz, 2H). $^{13}C\{^1H\}$ NMR (500 MHz, $CDCl_3$) δ 173.4 (*C*ON), 172.4 (*C*OO), 157.6 (*aromatic =C*),129.9 (*aromatic =C*H), 129.1 (*aromatic =C*H), 124.1 (*aromatic =C*), 120.8 (*aromatic =C*H), 110.5 (*aromatic =C*H), 55.5 (O*C*H_3), 52.5 (O*C*H_3), 48.9 (*C*H_2Ar), 41.2 (*C*H_2N), 36.1 (*C*H_2*C*O), 34.2 (*C*HCO). HRMS (ESI) calcd for $C_{14}H_{18}NO_4$ $[M+H]^+$ 264.1236. Found 264.1230.

Methyl-1-(2-methoxyphenylethyl)-5-oxopyrrolidine-3-carboxylate **1f.** Following the general procedure **A** the title product was purified by flash chromatography (*n*-pentane / EtOAc = 4:6) yielding lactam **1f** (0.86 mg, 98%) as yellow oil. Anal. calcd for $C_{14}H_{18}NO_4$: C, 64.97; H, 6.91; N, 5.05. Found: C, 64.47; H, 6.86; N, 5.16. IR, ν_{max} /cm^{-1} (neat): 1734 (COO), 1784 (CON). ^1H NMR (500 MHz, $CDCl_3$) δ 7.19 (t, *J* = 8.0 Hz, *aromatic* 1H), 7.11 (d, *J* = 7.5 Hz, *aromatic* 1H), 7.87-7.82 (m, *aromatic* 2H), 3.82 (s, 3H), 3.70 (s, 3H), 3.51-3.48 (m, 3H), 3.46-3.42 (m, 1H), 3.16-3.10 (m, 1H), 2.87-2.80 (m, 2H), 2.62 (qd, *J* = 16.9, 10.0 Hz, 2H). $^{13}C\{^1H\}$ NMR (126 MHz, $CDCl_3$) δ 173.3 (*C*ON), 172.2 (*C*OO), 157.6 (*aromatic =C*), 130.4 (*aromatic =C*H), 127.9 (*aromatic =C*H), 126.8 (*aromatic =C*), 120.5 (*aromatic =C*H), 110.3 (*aromatic =C*H), 55.3 (O*C*H_3), 52.4 (O*C*H_3), 49.5 (*C*H_2*C*H_2), 42.5 (*C*H_2N), 36.1 (*C*H_2*C*O), 34.1 (*C*HCO), 28.5 (*C*H_2Ar). HRMS (ESI) calcd for $C_{14}H_{19}NO_4$ $[M+H]^+$ 278.1392. Found 278.1389.

Methyl-1-cyclohexyl-5-oxopyrrolidine-3-carboxylate **1g**. Following the general procedure **A** the title product was purified by flash chromatography (*n*-pentane/ EtOAc = 4:6) yielding lactam **1g** (575 mg, 81%) as a tan oil, which solidified on standing. Anal. calcd for $C_{12}H_{19}NO_3$: C, 63.98; H, 8.50; N, 6.22. Found: C, 63.90; H, 8.57; N, 6.20. IR, ν_{max} /cm^{-1} (neat): 1730 (COO), 1667 (CON). ^1H NMR (500 MHz, $CDCl_3$) δ 3.96-3.89 (m, 1H), 3.72 (s, 3H), 3.58-3.52 (m, 2H), 3.21-3.15 (m, 1H), 1.84-1.75 (m, 2H), 1.71-1.64 (m, 3H), 1.41-1.30 (m, 4H), 1.15-1.01 (m, 1H). $^{13}C\{1H\}$ NMR (126 MHz, $CDCl_3$) δ 173.5 (*C*ON), 171.7 (*C*OO), 52.5 (O*C*H_3), 50.7 (*C*HN), 46.1 (*C*H_2N), 36.4 (*C*H_2*C*O), 34.8 (*C*HCO), 30.4 (*C*H_2), 30.2 (*C*H_2), 25.5 (2 (*C*H_2)), 25.4 (*C*H_2). HRMS (ESI) calcd for $C_{12}H_{20}NO_3$ $[M+H]^+$ 226.1443. Found 226.1438.

Methyl-1-p-methylbenzyl-5-oxopyrrolidine-3-carboxylate **1h.** Following general procedure **A** the title product was purified by flash chromatography (*n*-pentane/ EtOAc = 3:7) yielding lactam **1h** (670 mg, 86%) as a tan oil, which solidified on standing. Anal. calcd for $C_{14}H_{17}NO_3$: C, 68.00; H, 6.93; N, 5.66. Found: C, 68.02; H, 6.97; N, 5.65. IR, ν_{max}/cm^{-1} (neat):1729 (COO), 1669 (*C*ON). ^1H NMR (500 MHz, $CDCl_3$, δ ppm): 7.14-7.10 (m, *aromatic* 4H), 4.50 (AB, *J*= 14.1 Hz, 2H), 3.69 (s, 3H), 4.47-3.41 (m, 2H), 3.22 -3.15 (m, 1H), 2.72 (qd, *J* = 17.1, 8.7 Hz, 2H), 2.33 (s, 3H). $^{13}C\{^1H\}$ NMR (500 MHz, $CDCl_3$ δ, ppm): 173.3 (*C*ON), 172.3 (*C*OO), 137.6 (*aromatic* =C), 132.9 (*aromatic =C*), 129.5 (*aromatic* 2 (=*C*H)), 128.3 (*aromatic* 2 (=*C*H)), 52.5 (O*C*H_3), 48.5 (*C*H_2Ar), 46.3 (*C*H_2N), 35.9 (*C*H_2CO), 34.2 (*C*HCO), 21.2 (*C*H_3). HRMS (ESI) calcd for $C_{14}H_{17}NO_3Na$ $[M+Na]^+$ 270.1106. Found 270.1100.

Methyl-5-oxo-1-(4-phenylbutyl)-pyrrolidine-3-carboxylate **1i.** Following general procedure **A** the title product was purified by flash chromatography (*n*-pentane/ EtOAc = 1:9) yielding lactam **1i** (760 mg, 87%) as an orange oil. Anal. calcd for $C_{16}H_{21}NO_3$: C, 69.79; H, 7.69; N, 5.09. Found: C, 69.56; H, 7.81; N, 5.16. IR, ν_{max}/cm^{-1} (neat): 1733 (COO), 1682 (CON). ^1H NMR (500 MHz, $CDCl_3$) δ 7.28-7.25 (m, *aromatic* 2H), 7.18-7.14 (m, *aromatic* 3H), 3.72 (s, 3H), 4.58-3.49 (m, 2H), 3.35 -3.24 (m, 2H), 3.23-3.16 (m, 1H), 2.72-2.61 (m, 4H), 1.64-1.58 (m, 2H), 1.56-1.51 (m, 2H). $^{13}C\{1H\}$ NMR (500 MHz, $CDCl_3$) δ 173.3 (*C*ON), 172.3 (*C*OO), 142.0 (*aromatic* =C), 128.4 (*aromatic* 2 (=*C*H)), 128.4 (*aromatic* 2 (=*C*H)), 125.9 (*aromatic =C*H), 52.5 (O*C*H_3), 48.9 (*C*H_2N), 42.3 (*C*H_2N), 36.0 (*C*H_2CO), 36.4 (*C*H_2Ph), 34.2 (*C*HCO), 28.5 (*C*H_2), 26.6 (*C*H_2). HRMS (ESI) calcd for $C_{16}H_{21}NO_3$+K $[M+K]^+$ 314.1159. Found 314.1153.

Methyl 1-butyl-5-oxoxpyrrolidine-3-carboxylate **1j**.[34a] Following the procedure **A** the title product was purified by flash chromatography (*n*-pentane/ EtOAc = 1: 9) colourless oil **1j**

(560 mg, 88%). Anal. calcd for $C_{10}H_{18}NO_3$: C, 60.28; H, 7.69; N, 7.03. Found: C, 58.86, H, 8.60; N, 6.94. IR, ν_{max} /cm^{-1} (neat): 1734 (COO), 1681 (CON). ^{1}H NMR (500 MHz, $CDCl_3$) δ 3.70 (s, 3H), 3.60-3.51 (m, 2H), 3.25-3.21 (m, 1H), 3.23-3.16 (m, 2H), 2.69-2.59 (m, 2H), 1.49-1.34 (m, 2H), 1.31-1.24 (m, 2H), 0.90-0.87 (m, 3H). ^{13}C{1H} NMR (126 MHz, $CDCl_3$) δ 173.4 (*C*ON), 172.2 (*C*OO), 52.5 (O*C*H$_3$), 48.9 (*C*H$_2$N), 42.2 (*C*H$_2$N), 36.1 (*C*H$_2$CO), 34.3 (*C*HCO), 29.2 (*C*H$_2$-CH$_2$), 20.0 (CH$_2$-*C*H$_3$), 13.8 (*C*H$_3$). HRMS (ESI) calcd for $C_{10}H_{18}NO_3$ [M+H]$^+$: 200.1287. Found 200.1281.

***Methyl-1-(4-hydroxyphenyl)-5-oxopyrrolidine-3-carboxylate* 1k.** Following general procedure **A** the title product was obtained in 99% yield as a beige solid. Anal. calcd for $C_{14}H_{17}NO_4$: C, 63.87; H, 6.51; N, 5.32. Found: C, 63.81; H, 6.53; N, 5.37. IR, ν_{max}/cm^{-1} (neat): 1742 (COO), 1658 (*C*ON). ^{1}H NMR (500 MHz, $CDCl_3$) δ 7.03-7.01 (d, *J* = 8.5 Hz, *aromatic* 2H), 6.74-6.73 (m, *aromatic* 2H, 1 OH), 3.71 (s, 3H), 2.57-2.46 (m, 4H), 3.18-3.12 (m, 1H), 2.77 (t, *J* = 7.1 Hz, 2H), 2.65 (qd, *J* = 17.2, 8.6 Hz, 2H). ^{13}C{^{1}H} NMR (500 MHz, $CDCl_3$) δ 173.2 (*C*ON), 172.99 (*C*OO), 155.4 (*aromatic* =C), 129.7 (*aromatic* 2 (=C)), 129.3 (*aromatic* =*C*), 115.7 (*aromatic* =*C*H), 52.6 (O*C*H$_3$), 49.4 (*C*H$_2$N), 44.0 (*C*H$_2$N), 36.1 (*C*H$_2$CO), 34.2 (*C*H$_2$Ar), 32.7 (*C*HCO). HRMS (ESI) calcd for $C_{14}H_{17}NO_4$ +Na [M+Na]$^+$: 286.1055. Found 286.1049.

***Synthesis of methyl 1-benzylpyrrolidine-3-carboxylate 2a by reduction of pyrrolidin-2-one* 1a.** Et_3SiH (0.77 mmol, 120 µL, 6 equiv.) were added dropwise to a solution of pyrrolidin-2-one **1a** (0.13 mmol, 30 mg, 1 equiv.) and iridium catalyst[11] G2 (5 mol %) in 1,2-dichloroethane (~3.0 mL) at room temperature in the anhydrous conditions. The mixture was the allowed to slowly warm up to 60 °C using an oil bath. After that the reaction was stirred vigorously for 4 hours and monitored by TLC, at the end of the reaction the solvent was removed under vacuum and the crude product was purified by silica gel chromatography eluting with a mixture of *n*-pentane and ethyl acetate respectively (3/ 7) to afford the desired pyrrolidine **2a** (28 mg, 99%) as yellow oil. ^{1}H NMR (500 MHz, $CDCl_3$): δ 7.25-7.20 (m, *aromatic* 5H), 3.62 (s, 3H), 3.57 (s, 2H), 3.02-2.95 (m, 1H), 2.85 (t, *J* = 8.8 Hz, 1H), 2.68-2.64 (m, 1H), 2.56 (dd, *J* = 9.2, 7.1 Hz, 1H), 2.46 (q, *J* = 7.7 Hz, 1H), 2.06-2.02 (m, 2H). ^{13}C{1H} NMR (126 MHz, $CDCl_3$) δ 175.6 (*C*OO), 138.9 (*aromatic* =*C*), 128.9 (*aromatic* 2 (=*C*H)), 128.4 (*aromatic* 2 (=*C*H)), 127.1 (*aromatic* =*C*H), 60.2 (*C*H$_2$Ph), 56.8 (*C*H$_2$-*C*H$_2$), 53.9 (*C*H$_2$N), 51.9 (O*C*H3), 42.0 (*C*HCO), 27.7 (*C*H$_2$CH). HRMS (ESI) calcd for $C_{13}H_{18}NO_2$ [M+H]$^+$: 220.1338. Found 220.1332.

***Synthesis of methyl 1-(4-chlorobenzyl)pyrrolidine-3-carboxylate* 2b *by reduction of pyrrolidin-2-one* 1b.** Et_3SiH (0.89 mmol, 143 µL, 8 equiv.) were added dropwise to a solution of pyrrolidin-2-one **1b** (0.11 mmol, 30 mg, 1 equiv.) and iridium catalyst (5 mol%) in 1,2-dichloroethane (~3.0 mL) at room temperature in the anhydrous conditions. The mixture was allowed to slowly warm up to 60 °C using an oil bath. After that the reaction was stirred vigorously for 12 hours and monitored by TLC, at the end of the reaction the solvent was removed under vacuum and the crude product was purified by silica gel chromatography eluting a mixture of *n*-pentane and ethyl acetate respectively (4/ 6) to afford the desired pyrrolidine **2b** (28.3 mg, 98%) as an orange oil. ^{1}H NMR (500 MHz, $CDCl_3$): δ 7.29-7.24 (m, *aromatic* 4H), 3.68 (s, 3H), 3.59 (AB, *J* =13.3 Hz, 2H), 3.07-3.00 (m, 1H), 2.86 (t, *J* = 8.8 Hz, 1H), 2.69-2.66 (m, 1H), 2.64-2.61 (m, 1H), 2.52 (q, *J* = 7.6 Hz, 1H), 2.12-2.06 (m, 2H). ^{13}C{1H} NMR (126 MHz, $CDCl_3$) δ 175.5 (*C*OO), 137.9 (*aromatic* =*C*), 132.8 (*aromatic* =*C*Cl), 130.1 (*aromatic* 2 (=*C*H)), 128.5 (*aromatic* 2 (=*C*H)), 59.4 (*C*H$_2$Ar), 56.7 (*C*H$_2$-CH$_2$), 53.8 (*C*H$_2$N), 52.0 (O*C*H3), 42.0 (*C*HCO), 27.8 (*C*H$_2$CH). HRMS (ESI) calcd for $C_{13}H_{17}ClNO_2$ [M+H]$^+$: 254.0948. Found 254.0942.

***Synthesis of methyl 1-(4-methoxybenzyl)pyrrolidine-3-carboxylate 2c by reduction of pyrrolidin-2-one* 1c.** Et_3SiH (0.91 mmol, 146 µL, 8 equiv.) were added dropwise to a solution of pyrrolidin-2-one **1c** (0.11 mmol, 30 mg, 1 equiv.) and iridium catalyst (5 mol %) in 1,2-dichloroethane (~3.0 mL) at room temperature in the anhydrous conditions. The mixture was allowed to slowly warm up to 60 °C using an oil bath. After that the reaction was stirred vigorously for 24 hours and monitored by TLC, at the end of the reaction the solvent was removed under vacuum and the crude product was purified by silica gel chromatography eluting with a mixture of *n*-pentane and ethyl acetate respectively (3/ 7) to afford the desired pyrrolidine **2c** (28.2 mg, 99%) as an orange oil. ^{1}H NMR (500 MHz, $CDCl_3$) δ 7.23 (d, *J* = 8.6 Hz, *aromatic* 2H), 6.85 (d, *J* = 8.7 Hz, *aromatic* 2H), 3.80 (s, 3H), 3.68 (s, 3H), 3.56 (s, 2H), 3.06-3.00 (m, 1H), 2.89 (t, *J* = 8.9 Hz, 1H), 2.72-2.68 (m, 1H), 2.60-2.57 (m, 1H), 2.49 (q, *J* = 8.0 Hz, 1H), 2.11-2.07 (m, 2H). ^{13}C{^{1}H} NMR (126 MHz, $CDCl_3$): δ 175.7 (*C*OO), 158.8 (=*C*-OMe), 130.9 (*aromatic* =*C*), 130.1 (*aromatic* 2 (=*C*H)), 113.8 (*aromatic* 2 (=*C*H)), 59.5 (*C*H$_2$Ar), 56.7 (*C*H$_2$-CH$_2$), 55.4 (O*C*H$_3$), 53.7 (*C*H$_2$N), 52.0 (O*C*H3), 42.0 (*C*HCO), 27.7 (*C*H$_2$CH). HRMS (ESI) calcd for $C_{14}H_{20}NO_3$ [M+H]$^+$: 250.1443. Found 250.1438.

***Synthesis of methyl 1-(benzo[1,3-d]dioxol-5-ylmethyl)pyrrolidine-3-carboxylate* 2d *by reduction of pyrrolidin-2-one* 1d.** Et_3SiH (2.16 mmol, 346 µL, 20 equiv.) were added dropwise to a solution of pyrrolidin-2-one **1d** (0.11 mmol, 30 mg, 1 equiv.) and iridium catalyst (5 mol %) in 1,2-dichloroethane (~3.0 mL) at room temperature in the anhydrous conditions. The mixture was allowed to slowly warm up to 60 °C using an oil bath. After that the reaction was stirred vigorously for 38 hours and monitored by TLC, at the end of the reaction the solvent was removed under vacuum and the crude product was purified by silica gel chromatography eluting with a mixture of methanol and ethyl acetate respectively (0.5/ 10) to afford the desired pyrrolidine **2d** (28.3 mg, 98 %). ^{1}H NMR (500 MHz, $CDCl_3$): δ 6.83 (s, *aromatic* 1H), 6.73 (s, *aromatic* 2H), 5.92 (s, 2H), 3.67 (s, 3H), 3.51 (s, 2H), 3.05-2.99 (m, 1H), 2.88 (t, *J* = 8.8 Hz, 1H), 2.70-2.65 (m, 1H), 2.58 (dd, *J* = 9.4, 7.1 Hz, 1H), 2.48 (q, *J* = 7.8 Hz, 1H), 2.10-2.05 (m, 2H). ^{13}C{^{1}H} NMR (126 MHz, $CDCl_3$) δ 175.6 (*C*OO), 147.7 (*aromatic* =*C*-O), 146.6 (*aromatic* =*C*-O), 132.9 (*aromatic* =*C*), 121.9 (*aromatic* =*C*H), 109.3 (*aromatic* =*C*H), 108.0 (*aromatic* =*C*H), 100.9 (O-*C*H$_2$-O), 59.9 (*C*H$_2$Ar), 56.7 (*C*H$_2$-*C*H$_2$), 53.7 (*C*H$_2$N), 51.9 (O*C*H$_3$), 42.0 (*C*HCO), 27.7

(CH_2CH). HRMS (ESI) calcd for $C_{14}H_{18}NO_4$ $[M+H]^+$ 264.1236,. Found 264.1230.

***Synthesis of methyl 1-(2-methoxybenzyl)pyrrolidine-3-carboxylate* 2e *by reduction of pyrrolidin-2-one* 1e.** Et_3SiH (0.96 mmol, 155 μL, 8.5 equiv.) were added dropwise to a solution of pyrrolidin-2-one **1e** (0.11 mmol, 30 mg, 1 equiv.) and iridium catalyst (5 mol %) in 1,2-dichloroethane (~ 3.0 mL) at room temperature in the anhydrous conditions. The mixture was allowed to slowly warm up to 60 °C using an oil bath. After that the reaction was stirred vigorously for 32 hours and monitored by TLC, at the end of the reaction the solvent was removed under vacuum and the crude product was purified by silica gel chromatography eluting with ethyl acetate to afford the desired pyrrolidine **2e** (26.9 mg, 93%) as an orange oil. ^{1}H NMR (500 MHz, $CDCl_3$): δ 7.34-7.32 (*d*, *J* = 8.8 Hz, *aromatic* 1H), 7.23 (*t*, *J* = 8.6 Hz, *aromatic* 1H), 6.92 (*t*, *J* = 7.4 Hz, *aromatic* 1H), 6.86 (*d*, *J* = 8.2 Hz, *aromatic* 1H), 3.82 (*s*, 3H), 3.70 (*s*, 2H), 3.68 (*s*, 3H), 3.09-3.02 (*m*, 1H), 2.99 (*t*, *J* = 8.8 Hz, 1H), 2.81-2.77 (m, 1H), 2.68 (*dd*, *J* = 9.2, 7.2 Hz, 1H), 2.58 (*q*, *J* = 7.5 Hz, 1H), 2.12-2.07 (*m*, 2H). ^{13}C{^{1}H} NMR (126 MHz, $CDCl_3$) δ 175.7 (*C*OO), 157.9 (aromatic =*C*-OMe), 130.6 (aromatic =*C*H), 128.3 (aromatic =*C*H), 126.6 (aromatic =*C*), 120.5 (aromatic =*C*H), 110.5 (aromatic =*C*H), 56.7 (CH_2Ar), 55.5 (CH_2-CH_2), 53.7 (OCH_3), 53.2 (CH_2N), 51.9 (OCH3), 42.1 (*C*HCO), 27.7 (CH_2CH). HRMS (ESI) calcd for $C_{14}H_{20}NO_3$ $[M+H]^+$: 250.1443. Found 250.1438.

***Synthesis of methyl 1-(2-methoxyphenethyl)pyrrolidine-3-carobxylate* 2f *by reduction of pyrrolidin-2-one* 1f.** Et_3SiH (0.97 mmol, 155 μL, 6 equiv.) were added dropwise to a solution of pyrrolidin-2-one **1f** (0.11 mmol, 30 mg, 1 equiv.) and iridium catalyst (5 mol %) in 1,2-dichloroethane (~3.0 mL) at room temperature in the anhydrous conditions. The mixture was allowed to slowly warm up to 60 °C using an oil bath. After that the reaction was stirred vigorously for 20 hours and monitored by TLC, at the end of the reaction the solvent was removed under vacuum and the crude product was purified by silica gel chromatography eluting with ethyl acetate to afford the desired pyrrolidine **2f** (24.7 mg 87 %) as an orange oil. ^{1}H NMR (500 MHz, $CDCl_3$): δ 7.18 (t, *J* = 8.6 Hz, *aromatic* 1H), 7.14 (d, *J* = 8.8 Hz, *aromatic* 1H), 6.87 (t, *J* = 7.8 Hz, *aromatic* 1H), 6.84 (d, *J* = 8.1 Hz, *aromatic* 1H), 3.81 (s, 3H), 3.69 (s, 3H), 3.10-3.04 (m, 1H), 3.00 (t, *J* = 8.7 Hz, 1H), 2.85-2.81 (m, 2H), 2.80-2.76 (m,1H), 2.71-2.67 (m, 2H), 2.65-2.60 (m, 1H), 2.56 (q, *J* = 7.7 Hz, 1H), 2.12-2.07 (m, 2H); ^{13}C{^{1}H} NMR (126 MHz, $CDCl_3$): δ 175.6 (*C*OO), 157.6 (*aromatic* =*C*-OMe), 130.2 (*aromatic* =*C*H), 128.6 (*aromatic* =*C*), 127.4 (*aromatic* =*C*H), 120.5 (*aromatic* =*C*H), 110.3 (*aromatic* =*C*H), 56.9 (CH_2-CH_2), 56.2 (CH_2N), 55.3 (OCH_3), 54.0 (CH_2N), 52.0 (OCH3), 42.1 (*C*HCO), 30.0 (CH_2CH), 27.7 (CH_2Ar). HRMS (ESI) calcd for $C_{15}H_{22}NO_3$ $[M+H]^+$: 264.1600. Found 264.1594.

***Synthesis of methyl 1-cyclohexylpyrrolidine-3-carobxylate* 2g *by reduction of pyrrolidin-2-one* 1g.** Et_3SiH (3.32 mmol, 531 μL, 25 equiv.) were added dropwise to a solution of pyrrolidin-2-one **1g** (0.13 mmol, 30 mg, 1 equiv.) and iridium catalyst (5 mol%) in 1,2-dichloroethane (~ 3.0 mL) at room temperature in the anhydrous conditions. The mixture was allowed to slowly warm up to 60 °C using an oil bath. After that the reaction was stirred vigorously for 44 hours and monitored by TLC, at the end of the reaction the solvent was removed under vacuum and the crude product was purified by silica gel chromatography eluting with ethyl acetate to afford the desired pyrrolidine **2g** (21.1 mg, 75 %) as an orange oil. ^{1}H NMR (500 MHz, $CDCl_3$) δ 3.66 (s, 3H), 3.06-2.97 (m, 1H), 2.82-2.78 (m, 1H), 2.64-2.61 (m, 1H), 2.49 (q, *J* = 8.0 Hz 1H), 2.08-2.00 (m,3H), 1.92-1.90 (m, 2H), 1.74-1.69 (m, 2H), 1.60-1.55 (m, 1H), 1.24-1.16 (m, 5H). ^{13}C{^{1}H} NMR (126 MHz, $CDCl_3$) δ 175.6 (*C*OO), 63.5 (*C*HN), 54.4 (CH_2-CH_2), 51.9 (OCH_3), 51.3 (CH_2N), 41.7 (*C*HCO), 31.9 (CH_2CH), 27.5 (2 (CH_2)), 26.0 (2 (CH_2)), 25.1 (CH_2). HRMS (ESI) calcd for $C_{12}H_{22}NO_2$ $[M+H]^+$: 212.1651. Found 212.1645.

Synthesis of methyl 1-(4-methylbenzyl)pyrrolidine-3-carobxylate 2h by reduction of pyrrolidin-2-one 1h. Et_3SiH (0.48 mmol, 78 μL, 4 equiv.) were added dropwise to a solution of pyrrolidin-2-one **1h** (0.12 mmol, 30 mg, 1 equiv.) and iridium catalyst (5 mol %) in 1,2-dichloroethane (~3.0 mL) at room temperature in the anhydrous conditions. The mixture was allowed to slowly warm up to 60 °C using an oil bath. After that the reaction was stirred vigorously for 30 hours and monitored by TLC, at the end of the reaction the solvent was removed under vacuum and the crude product was purified by silica gel chromatography eluting with a mixture of *n*-pentane and ethyl acetate (5/5) to afford the desired pyrrolidine **2h** (28.1 mg, 99 %). ^{1}H NMR (500 MHz, $CDCl_3$): δ 7.21-7.11 (m, *aromatic* 4H), 3.68 (s, 3H), 3.59 (AX, *J* = 13.0 Hz, 2H), 3.07-3.00 (m, 1H), 2.92 (t, *J* = 8.8 Hz, 1H), 2.72-2.68 (m, 2H), 2.61-2.58 (m, 1H), 2.50 (q, *J* = 7.8 Hz, 1H), 2.33 (s, 3H), 2.11-2.06 (m, 2H). ^{13}C{^{1}H} NMR (126 MHz, $CDCl_3$): δ 175.7 (*C*OO), 136.7 (*aromatic* =*C*-Me), 135.8 (*aromatic* =*C*), 129.1 (*aromatic* 2 (=*C*H)), 128.9 (*aromatic* 2 (=*C*H)), 59.9 (CH_2Ar), 56.8 (CH_2-CH_2), 53.8 (CH_2N), 51.9 (OCH3), 42.1 (*C*HCO), 27.7 (CH_2CH), 21.2 (CH_3). HRMS (ESI) calcd for $C_{14}H_{20}NO_2$ $[M+H]^+$: 234.1494. Found 234.1488.

Synthesis of methyl 1-(4-phenylbutyl)pyrrolidine-3-carboxylate 2i by reduction of pyrrolidin-2-one 1i. Et_3SiH (0.52 mmol, 84 μL, 4 equiv.) were added dropwise to a solution of pyrrolidin-2-one **1i** (0.13 mmol, 36 mg, 1 equiv.) and iridium catalyst (5 mol %) in 1,2-dichloroethane (~3.0 mL) at room temperature in the anhydrous conditions. The mixture was allowed to slowly warm up to 60 °C using an oil bath. After that the reaction was stirred vigorously for 7 hours and monitored by TLC, at the end of the reaction the solvent was removed under vacuum and the crude product was purified by silica gel chromatography eluting with ethyl acetate to afford the desired pyrrolidine **2i** (34 mg, 100 %) as an orange oil. ^{1}H NMR (500 MHz, $CDCl_3$): δ 7.27-7.24 (m, *aromatic* 2H), 7.17-7.14 (m, *aromatic* 3H), 3.67 (s, 3H), 3.05-2.98 (m, 1H), 2.86 (t, *J* = 8.8 Hz, 1H), 2.68-2.57 (m, 4H), 2.49-2.38 (m, 3H), 2.09-2.04 (m, 2H), 1.67-1.61 (m, 2H), 1.56-1.50 (m, 2H). ^{13}C{^{1}H} NMR (126 MHz, $CDCl_3$): δ 175.6 (*C*OO), 142.5 (*aromatic* =*C*), 128.5 (*aromatic* 2 (=*C*H)), 128.4 (*aromatic* 2 (=*C*H)), 125.8 (*aromatic* =*C*H), 57.0 (CH_2N), 56.1 (CH_2-CH_2), 54.1 (CH_2N), 52.0 (OCH3), 42.0 (*C*HCO), 35.9 (CH_2Ph), 29.5

(CH_2CH), 28.6 (CH_2CH_2), 27.7 (CH_2CH_2). HRMS (ESI) calcd for $C_{16}H_{24}NO_2$ $[M+H]^+$: 262.1807. Found 282.1801.

***Synthesis of methyl -1-butylpyrrolidine-3-carboxylate* 2j *by reduction of pyrrolidin-2-one* 1j.** Et_3SiH (1.17 mmol, 187 µL, 6 equiv.) were added dropwise to a solution of pyrrolidin-2-one **1j** (0.2 mmol, 39 mg, 1 equiv.) and iridium catalyst (5 mol %) in 1,2-dichloroethane (~3.0 mL) at room temperature in the anhydrous conditions. The mixture was allowed to slowly warm up to 60 °C using an oil bath. After that the reaction was stirred vigorously for 18 hours and monitored by TLC, at the end of the reaction the solvent was removed under vacuum and the crude product was purified by silica gel chromatography eluting with ethyl acetate, during the remove of the solvent and after purification, the desired product was evaporated with the solvent (conversion: 94%) ^{1}H NMR (500 MHz, $CDCl_3$): δ 3.66 (s, 3H), 3.10-3.01 (m, 2H), 2.86-2.80 (m, 1H), 2.69 (dd, *J* = 9.2, 6.6 Hz ,1H,) 2.56-2.45 (m, 3H), 2.17-2.05 (m, 2H), 1.54-1.48 (m, 2H), 1.35-1.27 (m, 2H), 0.96-0.94 (m, 3H), 0.92-0.88 (m, 18H), 0.58-0.47 (m, 12H). $^{13}C\{^1H\}$ NMR (126 MHz, $CDCl_3$): δ 175.1 (*C*OO), 56.5 (*C*H_2-*C*H_2), 55.9 (*C*H_2N), 53.9 (*C*H_2N), 52.1 (O*C*H_3), 41.9 (*C*H_2), 30.5 (*C*HCO), 27.7 (*C*H_2), 20.7 (*C*H_2), 14.0 (*C*H_3), 6.8 (*C*H_2-Si), 6.5 (*C*H_3). HRMS (ESI) calcd for $C_{10}H_{20}NO_2$ $[M+H]^+$: 186.1494. Found 186.1489.

***Synthesis of a mixture of methyl 1-(4-triethylsilyloxyphenethyl)pyrrolidine-3-carboxylate 2k and 3-(methoxy(triethylsilyloxy)methyl)-1-(4-triethylsilyloxyphenethyl)pyrrolidine 2k' by reduction of pyrrilidin-2-one 1k*.** Et_3SiH (2.05 mmol, 238 µL, 18 equiv.) were added dropwise to a solution of pyrrolidin-2-one **1k** (0.11 mmol, 30 mg, 1 equiv.) and iridium catalyst (5 mol %) in 1,2-dichloroethane (~3.0 mL) at room temperature in the anhydrous conditions. The mixture was allowed to slowly warm up to 60 °C using an oil bath. After that the reaction was stirred vigorously for 16 hours and monitored by TLC, at the end of the reaction the solvent was removed under vacuum and the crude products were purified and separated by silica gel chromatography eluting with ethyl acetate to afford the mixture of **2k** and **2k'** with conversion respectively 61 % and 39 %.

***Methyl 1-(4-triethylsilyloxyphenethyl)pyrrolidine-3-carboxylate 2k and 3-(methoxy(triethylsilyloxy)methyl)-1-(4-triethylsilyloxyphenethyl)pyrrolidine 2k'*.** ^{1}H NMR (500 MHz, $CDCl_3$) δ 7.05-7.03 (m, *aromatic* 4H), 6.77-6.74 (m, *aromatic* 3H), 4.61 (dd, *J* = 7.9, 6.4 Hz, 1H), 3.69 (s, 3H), 3.31 (s, 2H), 3.05 (m, *J* = 31.5 Hz, 1H), 2.94 (t, *J* = 8.8 Hz, 1H), 2.81-2.62 (m, 10H), 2.58-2.53 (m, 1H), 2.13-2.08 (m, 2H), 1.95-1.86 (m, 1H), 1.74-1.62 (m, 1H), 0.91 (t, *J* = 8.1 Hz, 36H), 0.75-0.70 (m, 9H), 0.52 (q, *J* = 8.0 Hz, 30H); $^{13}C\{1H\}$ NMR (126 MHz, CDCl3) δ 175.6 (COO), 154.0 (*aromatic* =C-O-), 153.9 (*aromatic* 2 (=C-O-)), 133.0 (*aromatic* =C), 132.9 (*aromatic* 2 (=C)), 129.6 (*aromatic* 4 (=CH)), 129.6 (*aromatic* 2 (=CH)), 119.9 (*aromatic* 4 (=CH)), 119.9 (*aromatic* 2 (=CH)), 101.4 (HC*), 101.3 (HC*), 58.5 (*C*H_2-CH_2), 58.5 (CH_2-*C*H_2), 58.2 (*C*H_2-CH_2), 56.9 (*C*H_2N), 56.1 (*C*H_2N), 55.2 (*C*H_2N), 54.3 (*C*H_2N), 54.1 (*C*H_2N), 53.7 (*C*H_2N), 53.3 (O*C*H_3), 52.0 (O*C*H_3), 43.7 (O*C*H_3), 42.1 (*C*HCO), 34.9 (*C*H_2Ar), 34.7 (*C*H_2Ar), 34.6 (*C*H_2Ar), 27.8 (*C*H_2CH), 26.9 (CH_2*C*H), 25.9 (*C*H_2CH) 7.0 (*C*H_2), 6.9 (*C*H_2), 6.8 (*C*H_2), 6.6 (*C*H_3), 5.3 (*C*H_3), 5.1 (*C*H_3). HRMS (ESI) calcd for $C_{20}H_{34}NO_3Si$ $[M+H]^+$ 364.2308, found 364.2302. HRMS (ESI) calcd for $C_{26}H_{50}NO_3Si_2$ $[M+H]^+$ 480.3329, found 480.3327.

General procedure B for the synthesis of enamides 4. The enamides **4** were prepared according to a literature procedure[35] with minor modifications. To a solution of dimethyl-α-(bromomethyl)fumarate (8.44 mmol, 2 g, 1 equiv.) in boiling bromobenzene (~10 mL) were added dropwise the appropriately amine (16.87 mmol, 2 equiv.), the reaction was stirred for 20 minutes, then cooled, filtered and the solvent was removed under vacuum. The crude product was purified by silica gel chromatography. Recrystallization from a mixture of diethyl ether and hexane respectively (4/6) gave desired enamides **4a-c**.

***Methyl 1-benzyl-5-oxo-4,5-dihydro-1H-pyrrole-3-carboxylate* 4a.** Following General procedure **B** the title product was purified by flash chromatography (petroleum ether/ diethyl ether: 5/5). Recrystallization from a mixture of *n*-hexane and petroleum ether respectively (6/4) gave desired enamide **4a** as a white solid (1.37 g, 70%). Anal. calcd for $C_{13}H_{13}NO_3$: C, 67.52; H, 5.67; N, 6.06. Found: C, 67.48; H, 5.95; N, 5.94. IR, ν_{max} / cm^{-1} (neat): 1722 (COO), 1695 CON), 1619 (C=C). ^{1}H NMR (500 MHz, $CDCl_3$) *δ* 7.36-7.22 (6H, 5 *aromatic* H and 1 enamide H), 4.65 (s, 2H), 3.69 (s, 3H), 3.35 (d, *J* = 2.0 Hz, 2H). $^{13}C\{^1H\}$ NMR (126 MHz, $CDCl_3$) δ 175.9 (*C*ON), 163.5 (*C*OO), 142.8 (=*C*H-N), 135.8 (*aromatic* =*C*),129.1 (*aromatic* 2 (=*C*H)), 128.3 (*aromatic* =*C*H), 128.1 (*aromatic* 2 (=*C*H)), 108.96 (=*C*), 51.4 (*C*H_2Ph), 46.1 (O*C*H_3), 36.4 (*C*H_2CO). HRMS (ESI) calcd for $C_{13}H_{13}NO_3$+Na $[M+Na]^+$: 254.0793. Found 254.0782.

***Methyl 1-cyclohexyl-5-oxo-4,5-dihydro-1H-pyrrole-3-carboxylate* 4b.**[36] Following General procedure B the title product was purified by flash chromatography (*n*-pentane/ EtOAc = 8: 2). Recrystallization from a mixture of *n*-hexane and petroleum ether respectively (6/ 4) gave desired enamide **4b** as a white solid (0.98 g, 52%). Anal. calcd for $C_{12}H_{17}NO_3$: C, 64.55; H, 7.67; N, 6.27. Found: C, 64.63; H, 5.69; N, 6.34. IR, ν_{max} / cm^{-1} (neat): 1720 (COO), 1695 (CON), 1620 (C=C). ^{1}H NMR (500 MHz, $CDCl_3$) δ 7.49 (s, enamide1H), 3.99-3.90 (m, 1H), 3.73 (s, 3H), 3.31 (d, *J* = 2.0 Hz, 2H), 1.89-1.79 (m, 4H), 1.43-1.67 (m,1H) 1.43-1.30 (m, 4H), 1.19-1.10 (m, 1H). $^{13}C\{^1H\}$ NMR (126 MHz, $CDCl_3$) δ 175.8 (*C*ON), 163.8 (*C*OO) 141.1 (=*C*-N), 108.5 (=*C*), 51.4 (*C*HN), 51.0 (O*C*H_3), 37.0 (*C*H_2), 32.4 (2 (*C*H_2)), 25.5 (2 (*C*H_2)), 25.3 (*C*H_2). HRMS (ESI) calcd for $C_{12}H_{17}NO_3$+Na $[M+Na]^+$: 246.1106. Found 246.1101.

***Methyl 1-phenethyl-5-oxo-4,5-dihydro-1H-pyrrole-3-carboxylate* 4c.** Following General procedure **B** the title product was purified by flash chromatography (petroleum ether/ diethyl ether = 5:5). Recrystallization from a mixture of diethyl ether and petroleum ether respectively (3/ 7) gave desired enamide **4c** as a beige solid (0.95 g, 55%). Anal. calcd

for $C_{14}H_{15}NO_3$: C, 68.56; H, 6.16; N, 5.71. Found: C, 68.37; H, 6.14; N, 5.81. IR, ν_{max} / cm^{-1} (neat): 1701 (COO), 1685 (CON), 1616 (C=C).^{1}H NMR (500 MHz, $CDCl_3$) δ 7.32-7.15 (m, *aromatic* 5H and enamide 1H), 3.76-3.73 (m, 2H), 3.72 (s, 3H), 3.28 (d, *J* = 2 Hz, 2H), 2.91 (t, *J* = 7.3 Hz, 2H); ^{13}C{^{1}H} NMR (126 MHz, $CDCl_3$) δ 176.1 (*C*ON), 163.6 (*C*OO), 143.5 (=*C*-N), 137.7 (*aromatic* =*C*), 128.9 (*aromatic* 2 (=*C*H)), 128.8 (*aromatic* 2 (=*C*H)), 127.1 (*aromatic* =*C*H), 108.3 (=*C*), 51.5 (O*C*H3), 44.2 (*C*H_2N), 36.5 (*C*H_2CO), 35.4 (*C*H_2Ph). HRMS (ESI) calcd for $C_{14}H_{15}NNaO_3$ $[M+Na]^+$: 268.0950. Found 268.0944.

***Procedure for the synthesis of 1-benzyl-4-((triethylsilyloxy)methylene)pyrrolidin-2-one 5a by reduction of enamide* 4a**. Et_3SiH (1.04 mmol, 166 µL, 8 equiv.) was added dropwise (1 equivalent per hour) to a solution of enamide **4a** (0.13 mmol, 30 mg, 1 equiv.) and iridium catalyst (5 mol%) in 1,2- dichloroethane (~3 mL) at room temperature in the anhydrous conditions. The mixture was then allowed to slowly warm up to 60 °C using an oil bath. After that the reaction was stirred vigorously for 9 hours and monitored by TLC. At the end of the reaction the solvent was removed under vacuum and the crude product was purified by silica gel chromatography eluting with a mixture of *n*-pentane and ethyl acetate respectively (7 /3) to afford a mixture of **5a** and [**IrH**] [14b] as a yellow oil. ^{1}H NMR (500 MHz, $CDCl_3$) δ 7.34-7.23 (m, 5H, ArH), 6.06 (quint, *J* = 1.7 Hz, 1H), 4.61 (s, 2H), 4.45 (d, *J* = 1.6 Hz, 2H), 3.81 (d, *J* = 1.7 Hz, 2H), 0.93 (t, *J* = 8.0 Hz, 9H), 0.6 (q, *J* = 7.8 Hz, 6H). ^{13}C{^{1}H} NMR (126 MHz, $CDCl_3$) δ 171.5 (*C*ON), 159.0 (=*C*-H), 137.52 (aromatic =*C*), 128.9 (aromatic 2 (=*C*H)), 128.1 (aromatic 2 (=*C*H)), 127.6 (aromatic =*C*H), 121.5 (=*C*), 60.3 (*C*H_2N), 51.7 (*C*H_2Ph), 46.1 (*C*H_2CO), 6.8 (3 (CH_3*C*H_2)Si), 4.4 (3 (*C*$H_3$$CH_2$)Si). HRMS (ESI) calcd for $C_{18}H_{28}NO_2Si$ $[M+H]^+$: 318.1889. Found 318.1884.

Procedure for the synthesis of 1-cyclohexyl-4-((triethylsilyloxy)methylene)pyrrolidin-2-one 5b by reduction of enamide 4b. Et_3SiH (0.67 mmol, 78 µL, 5 equiv.) was added dropwise (1 equivalent per hour) to a solution of enamide **4b** (0.13 mmol, 30 mg, 1 equiv.) and iridium catalyst (5 mol%) in 1,2- dichloroethane (~3 mL) at room temperature in the anhydrous conditions. The mixture was then allowed to slowly warm up to 60 °C using an oil bath. After that the reaction was stirred vigorously for 6 hours and monitored by TLC. At the end of the reaction the solvent was removed under vacuum and the crude product was purified by silica gel chromatography eluting with a mixture of *n*-pentane and ethyl acetate respectively (7 /3) to afford a mixture of **5b** as an orange oil and [**IrH**]. ^{1}H NMR (500 MHz, $CDCl_3$) δ 5.98 (quint, *J* = 1.6 Hz, 1H), 4.49 (d, *J* = 1.7 Hz, 2H), 4.03-3.97 (m,1 H), 3.89 (d, *J* = 1.7 Hz, 2H), 1.85-1.77 (m, 4H), 1.74-1.63 (m, 2H), 1.44-1.30 (m, 4H), 0.96 (t, *J* = 7.9 Hz, 9H), 0.62 (q, *J* = 8.1 Hz, 6H). ^{13}C{^{1}H} NMR (126 MHz, $CDCl_3$) δ 170.9 (*C*ON), 158.2 (=*C*-H), 122.0 (=*C*), 60.4 (*C*HN), 50.3 (CH_2O), 48.4 (CH_2N), 31.8 (2 (CH_2)), 25.7 (2 (CH_2)), 25.6 (CH_2), 6.8 (3 (CH_3*C*H_2)Si), 4.5 (3 (*C*$H_3$$CH_2$)Si). HRMS (ESI) calcd for $C_{17}H_{32}NO_2Si$ $[M+H]^+$: 310.2202. Found 310.2203.

Procedure for the synthesis of 1-phenethyl-4-((triethylsilyloxy)methylene)pyrrolidin-2-one 5c by reduction of enamide 4c. Et_3SiH (0.73 mmol, 85 µL, 6 equiv.) was added dropwise (1 equivalent per hour) to a solution of enamide **4c** (0.12 mmol, 30 mg, 1 equiv.) and iridium catalyst G2 (5 mol%) in 1,2- dichloroethane (~3 mL) at room temperature in the anhydrous conditions. The mixture was then allowed to slowly warm up to 60 °C using an oil bath. After that the reaction was stirred vigorously for 7 hours and monitored by TLC. At the end of the reaction the solvent was removed under vacuum and the crude product was purified by silica gel chromatography eluting with a mixture of *n*-pentane and ethyl acetate respectively (6/4) to afford a mixture of **5c** as a orange oil and [**IrH**]. ^{1}H NMR (500 MHz, $CDCl_3$) δ 5.98 (quint, *J* = 1.6 Hz, 1H), 4.42 (d, *J* = 1.7 Hz, 2H), 3.72 (d, *J* = 1.7 Hz, 2H), 3.68 (t, *J* = 7.3 Hz, 2H), 2.89 (t, *J* = 7.3 Hz, 2H), 0.94 (t, *J* = 8.0 Hz, 9H), 0.60 (q, *J* = 7.9 Hz, 6H). ^{13}C{^{1}H} NMR (126 MHz, $CDCl_3$) δ 171.5 (*C*ON), 158.6 (=*C*H), 139.0 (*aromatic* =*C*), 128.8 (*aromatic* (2 (=CH)), 128.7 (*aromatic* (2 (=*C*H)), 126.6 (*aromatic* =*C*H), 121.7 (=C), 60.2 (*C*H_2N), 53.0 (*C*H_2-CO), 43.8 (*C*H_2-Ph), 35.2 (*C*H_2N),6.8 (3 (*C*H_2)), 4.5 (3 (*C*H_3)). HRMS (ESI) calcd for $C_{19}H_{30}NO_2Si$ $[M+H]^+$: 354.1865. Found 354.1860.

***Procedure for the synthesis of methyl 1-benzyl-4-methoxy-5-oxopyrrolidine-3-carboxylate* 7**.[18] Benzylamine (1.58 mmol, 1 equiv.) was added dropwise to a solution of dimethyl 2-methoxy-3-methylene succinate **6**[37] (0.3 g, 1.58 mmol) in methanol (~6 mL) in the anhydrous conditions. The mixture was then stirred vigorously for 10 hours at room temperature and monitored by TLC, at the end of the reaction the solvent was removed and under vacuum and the crude product was purified by silica gel chromatography eluting with a mixture of diethyl ether and petroleum ether respectively (8/ 2) to afford the lactam **7** as a white solid in 74 % yield. Anal. calcd for $C_{14}H_{17}NO_4$: C, 63.87; H, 6.51; N, 5.32; Found: C, 63.86; H, 6.59; N, 5.35. IR, ν_{max} / cm^{-1} (neat): 1741 (COO), 1696 (CON). ^{1}H NMR (500 MHz, $CDCl_3$) δ 7.35-7.23 (m, *aromatic* 5H), 4.48 (s, 2H), 4.08 (d, *J* = 7.3 Hz, 2H), 3.70 (s, 3H), 3.66 (dd, *J* = 10.1, 6.4 Hz, 1H), 3.61 (s, 3H), 3.36-3.32 (m, 1H), 3.25 (dd, *J* = 10.1, 7.8 Hz, 1H). ^{13}C{^{1}H} NMR (126 MHz, $CDCl_3$) δ 170.1 (COO), 169.7 (*C*ON), 135.7 (*aromatic* =C), 128.9 (*aromatic* 2 (=*C*H)), 128.3 (*aromatic* 2 (=*C*H)), 127.9 (*aromatic* =*C*H), 78.9 (*C*HOMe), 59.4 (O*C*H_3), 52.3 (O*C*H_3), 46.7 (*C*H_2Ph), 45.7 (*C*H_2N), 42.9 (*C*HCO). HRMS (ESI) calcd for $C_{14}H_{17}KNO_4$ $[M+K]^+$ 302.0795. Found 302.0789.

***Synthesis of a mixture of* 8 *and* 8' *by reduction of lactam* 7.** Et_3SiH (0.91 mmol, 146 µL, 8 equiv.) was added dropwise to a solution of lactam **7** (0.11 mmol, 30 mg, 1 equiv.) and iridium catalyst (5 mol%) in 1,2-dichloroethane (~ 3 mL) at room temperature in the anhydrous conditions. The mixture was then allowed to slowly warm up to 60 °C using an oil bath. After that the reaction was stirred vigorously for 21 hours and monitored by TLC. At the end of the reaction the solvent was removed under vacuum and the crude product was purified and separated by silica gel chromatography eluting with ethyl acetate to afford a mixture of **8** and **8'**.

***Methyl 1-benzyl-4-methoxypyrrolidine-3-carboxylates* 8.** The title product was isolated as a yellow oil in 38 % of conversion. ^{1}H NMR (500 MHz, $CDCl_3$) δ 7.2-7.17 (m, 5H, *aromatic* H), 4.04 (ddd, *J* = 7.8, 5.5, 4.5 Hz, 1H), 3.65 (s, 1H), 3.64-3.60 (m, 1H), 3.24 (s, 1H), 3.17 (q, *J* = 8.1 Hz, 1H), 3.04 (dd, *J* = 10.0, 5.5 Hz, 1H), 2.91- 2.84 (m, 2H), 2.46 (dd, *J* = 10.0, 4.5 Hz, 1H). ^{13}C{^{1}H} NMR (126 MHz, $CDCl_3$) δ 171.1 (*C*OO), 138.8 (=*C*), 129.0 (*aromatic* 2 (=*C*H)), 128.4 (*aromatic* 2 (=*C*H)), 127.2 (*aromatic* =*C*H), 81.1 (*C*-OMe), 60.5 (CH_2N), 59.0 (CH_2N), 58.0 (O*C*H_3), 54.2 (O*C*H_3), 51.8 (*C*H_2-CH), 48.3 (*C*HCO). HRMS (ESI) calcd for $C_{14}H_{20}NO_3$ $[M+H]^+$ 250.1443. Found 250.1438.

1-Benzyl-3-methoxy-4-(methoxy((triethylsilyl)oxy)methyl) pyrrolidine 8'. The title product was isolated as a yellow oil in 62 % of conversion. ^{1}H NMR (500 MHz, $CDCl_3$) δ 7.34-7.29 (m, 4H, *aromatic* H), 7.25-7.22 (m, 1H, *aromatic* H), 4.99 (d, *J* = 8.1 Hz, 1H), 3.78 (m, 1H), 3.72-3.69 (m, 2H), 3.28 (s, 3H), 3.24 (s, 3H), 2.89 (dd, *J* = 10.8, 4.5 Hz, 0H), 2.80 (t, *J* = 8.8 Hz, 1H), 2.69 (dd, *J* = 10.7, 2.4 Hz, 1H), 2.64 (t, *J* = 9.7 Hz, 1H), 2.51-2.45 (m, 1H), 0.98 (t, *J* = 8.0 Hz, 10H), 0.66 (q, *J* = 8.0 Hz, 5H). ^{13}C{^{1}H} NMR (126 MHz, $CDCl_3$) δ 139.3 (=*C*), 128.9 ((*aromatic* 2 (=*C*H)), 128.4 ((*aromatic* 2 (=*C*H)), 127.0 (*aromatic* =*C*H), 97.4 (*aromatic* =*C*H), 80.8 (*C*HOMe), 61.3 (CH_2N), 58.3 (CH_2N), 56.5 (O*C*H_3), 53.7 (O*C*H_3), 52.4 (CH_2N), 49.3 (*C*HCO), 7.0 (CH_2), 5.2 (CH_3). HRMS (ESI) calcd for $C_{20}H_{36}NO_3Si$ $[M+H]^+$ 366.12464. Found 366.2459.

Procedure for the ^{1}H NMR monitoring of reactions in sealed J-Young tubes. A clean dry J-Young NMR tube was loaded with the Ir-catalyst (2 mg, 1.42 μmol, 2 mol%), methyl-1-benzyl-5-oxo-pyrrolidine-3-carboxylate (**1a**) (17 mg, 0.073 mmol) and 1,3,5-tri-tert-butylbenzene (5.2 mg, 0.021 mmol) used as NMR standard reference for the quantification. To this mixture, 0.5 mL of dry CD_2Cl_2 was transferred and maintained under argon atmosphere. The NMR tube was swiftly cooled down to ~ -50°C. $HSiEt_3$ (68 μL, 0.42 mmol) was added to the cooled solution, which was subsequently tightly sealed and set for NMR analysis. ^{1}H NMR data acquisition was carried out with a Bruker AV-400 MHz NMR spectrometer at 298 K. Each spectrum was collected by 1D ^{1}H pulse program with a 30° hard pulse of 2.42 μs length in 4 scans with 2 s delay time after every scan. A 60 s delay was set between each spectrum. The spectra were collected and processed using an advanced plug-in of MestRe Nova software[19] requiring preliminary peaks assignment of relevant signals, which matched reported data. The 1D free induction decay of each spectrum at the respective data point was processed, and the products and the starting material were quantified based on the concentration of the NMR internal standard using the kinetic module of the MestRe[19] software.

Identification of intermediates 1a' and 2a'. The reaction was run in a sealed J-Young NMR sample tube using the above-explained procedure till the consumption **1a** to give the maximum **1a'** proton peak in the monitored NMR spectroscopy. The sample tube was quickly removed from the magnet and frozen to arrest any further progress of the reaction. Reactive intermediates were characterized primarily by NMR spectroscopy in a precooled probe of a NMR spectrometer at 213 K. Each spectrum was collected by 1D ^{1}H pulse program with a 30° hard pulse of 4.33 μs length in 32 scans with 3 s delay time after every scan. ^{1}H and ^{13}C NMR spectra were thus captured at the optimal formation of **1a'**. The NMR tube was further warmed to room temperature to reach reaction's completion. The resulting medium containing **2a'** was analyzed by high resolution mass spectroscopy using electrospray ionisation (ESI) by directly injecting the reaction mixture into the mass spectrometer's probe. Intermediate **1a'**: ^{1}H NMR (600 MHz, CD_2Cl_2): δ 7.78-6.51 (m, *aromatic* 5H), 4.84-4.73 (m, 1H), 3.60 (s, 2H), 3.65 (s, 3H), 3.00 (m, 1H), 3.01-2.98 (m, 1H), 2.88-2.82 (m, 1H), 2.69 (d, *J* = 9.7 Hz, 1H), 2.36-2.26 (m, 1H), 0.93 (t, *J* = 8.0 Hz, 9H), 0.55 (qd, *J* = 7.9, 3.2 Hz, 6H). ^{13}C {^{1}H} NMR (151 MHz, CD_2Cl_2): δ 175.5 (*C*OO), 138.8 (*aromatic* =C), 128.10 (*aromatic* 2 (=CH)), 127.8 (*aromatic* 2 (=*C*H)), 126.5 (*aromatic* =CH), 87.2 (*C*O$SiEt_3$), 53.0 (CH_2Ph), 51.8 (O*C*H_3), 51.03 (CH_2N), 39.14 (*C*HCO), 37.9 (CH_2COSiEt_3), 6.6 (*Si*CH_2), 5.62 (CH_3-CH_2). No HRMS was collected for **1a**' for it was very short-lived in the conditions of the catalysis. Compound **2a'**: ^{1}H NMR (500 MHz, $C_2D_4Cl_2$): δ 7.35-7.28 (m, *aromatic* 5H), 4.61-4.59 (m, 1H), 3.60 (m, 2H), 3.27 (s, 3H), 2.58-2.51 (m, 1H), 2.50-2.43 (m, 1H), 2.42-2.36 (m, 2H), 2.09-2.03 (m, 1H), 1.77-1.90 (m, 1H), 1.70-1.58 (m, 1H), 1.09-0.91 (m, 9H), 0.71-0.51 (m, 6H); ^{13}C NMR (126 MHz, $C_2D_4Cl_2$) δ: 149.8 (*aromatic* =C), 128.6 (*aromatic* 2 (=*C*H)), 128.5 (*aromatic* 2 (=*C*H)), 119.3 (*aromatic* (=*C*H), 101.2 (*C*HOSi), 60.2 (CH_2Ph), 56.2 (CH_2-CH_2), 54.1 (CH_2N), 53.91 (O*C*H_3), 43.7 (*C*HCH), 34.8 (CH_2CH), 8.0 (CH_2SiO), 6.7 (CH_3CH_2). HRMS (ESI) calcd $C_{19}H_{34}NO_2Si$ $[M+H]^+$ 336.2359 m/z. Found: 336.2332 m/z.

Computational details. ***a) DFT-D computations.*** Geometry optimization of the reactants, intermediates, transition states, and products were performed using the SCM-ADF2019.01[38] package, at the Density Functional Theory (DFT) level. The Perdew-Burke-Ernzerhof (PBE)[39] functional augmented with Grimme's dispersion corrections with the electronegativity equilibrium model (DFT-D4(EEQ))[40] was used in all geometry optimizations. Unless otherwise stated, all geometry computations were carried out using scalar relativistic effects with *ad hoc* all-electron single polarization functions triple-ζ Slater-type basis set (TZP)[41]. Solvation was treated by the Conductor-like Screening Model (COSMO)[42] procedure assuming 1,2-dichloroethane as a solvent and predefined Allinger atomic radii. Geometry optimization by energy gradient minimization were carried out in all cases with integration grid accuracy "normal".[43] Transition states were submitted to the Intrinsic Reaction Coordinate (IRC)[44] procedure to verify the connection to their reactive complexes and products. Vibrational modes were analytically computed to verify that the optimized geometries were related to energy minima or to transition states. ***b) IBSI computations.*** Intrinsic Bond Strength Index (IBSI) of the key atom pairs were computed using the IGMPLOT program[25b,33] using gaussian-type wavefunctions obtained from single-point calculations with the PBE functional[39] augmented with Grimme's correction to the dispersion with a Becke-Johnson damping function[45](PBE-D3(BJ)), scalar relativistic effects with the balanced Karlsruhe 2nd generation default triple-ζ valence plus polarization (def2-TZVP) basis set[46] and solvation model based on density (SMD)[47] simulating dichloroethane (ε= 10.36) as a solvent on the previ-

ously optimized geometry using the ORCA program system[48] version 4.1.1.

Supporting Information

Analytical data and spectra of relevant compounds, details on kinetic monitoring experiments, computational details including energies of stationary geometries, details of the IGM analyses with IGM plots and enhanced figures of the optimized geometries of key adducts. Optimized geometries of relevant compounds are provided as a compilation of coordinates under the .xyz format. CCDC 2283430-2283433 contain the supplementary crystallographic data for this paper. These data can be obtained free of charge via www.ccdc.cam.ac.uk/data_request/cif, or by emailing data_request@ccdc.cam.ac.uk, or by contacting The Cambridge Crystallographic Data Centre, 12 Union Road, Cambridge CB2 1EZ, UK; fax: +44 1223 336033.

AUTHOR INFORMATION

Corresponding Author

* Dr Jean-Pierre Djukic, Email: djukic@unistra.fr;
Dr Aïcha Arfaoui, Email: aicha.arfaoui@fst.utm.tn.

Author Contributions

The manuscript was written through contributions of all authors. All authors have given approval to the final version of the manuscript.

ACKNOWLEDGMENT

The CNRS and the University of Strasbourg are thanked for their financial support. The Faculty of Science of the University al Manar is thanked for a stipend allocated to H.K. for an extended stay at the University of Strasbourg. The GENCI-IDRISS and mesocentre of the University of Strasbourg are acknowledged for the allocated computing time slots. C.M.G. gratefully acknowledges the support of the Agence Nationale de la Recherche through a doctoral position (project Dip-NMR-19-CE42-0015-02). S.F.A.M. gratefully acknowledged the support provided through a associate research position by a grant of the Jean-Marie Lehn Foundation. Y.C. is grateful to the CCUS (grant g2023a74c) and the GENCI-IDRIS (grant AD010812469R2) for providing access to the local Unistra and nation computational facilites, respectively.

The authors declare no competing financial interests

REFERENCES

(1) Preat, J.; Michaux, C.; André, J.-M.; Perpète, E. A., Pyrrolidine-based dye-sensitized solar cells: A time-dependent density functional theory investigation of the excited state electronic properties *Int. J. Quant. Chem.* **2012**, *112*, 2072-2084.

(2) Li Petri, G.; Raimondi, M. V.; Spanò, V.; Holl, R.; Barraja, P.; Montalbano, A., Pyrrolidine in Drug Discovery: A Versatile Scaffold for Novel Biologically Active Compounds *Top. Curr. Chem.* **2021**, *379*, 34.

(3) Eastgate, M. D.; Schmidt, M. A.; Fandrick, K. R., On the design of complex drug candidate syntheses in the pharmaceutical industry *Nature Rev. Chem.* **2017**, *1*, 0016.

(4) Brown, H. C.; Weissman, P. M.; Yoon, N. M., Selective Reductions. IX. Reaction of Lithium Aluminum Hydride with Selected Organic Compounds Containing Representative Functional Groups1 *J. Am. Chem. Soc.* **1966**, *88*, 1458-1463.

(5) Kornet, M. J.; Thio, P. A.; Tan, S. I., Borane reduction of amido esters *J. Org. Chem.* **1968**, *33*, 3637-3639.

(6) (a) Coetzee, J.; Dodds, D. L.; Klankermayer, J.; Brosinski, S.; Leitner, W.; Slawin, A. M. Z.; Cole-Hamilton, D. J., Homogeneous Catalytic Hydrogenation of Amides to Amines *Chem. Eur. J.* **2013**, *19*, 11039-11050. (b) Okamoto, K.; Nagahara, S.; Imada, Y.; Narita, R.; Kitano, Y.; Chiba, K., Hydrosilane-Mediated Electrochemical Reduction of Amides *J. Org. Chem.* **2021**, *86*, 15992-16000.

(7) (a) Seyden-Penne, J. *Reductions by the Alumino- and Borohydrides in Organic Synthesis, 2nd Edition*; Wiley VCH, 1997. (b) W. Gribble, G., Sodium borohydride in carboxylic acid media: a phenomenal reduction system *Chem. Soc. Rev.* **1998**, *27*, 395-404.

(8) Xiang, S.-H.; Xu, J.; Yuan, H.-Q.; Huang, P.-Q., Amide Activation by Tf_2O: Reduction of Amides to Amines by $NaBH_4$ under Mild Conditions *Synlett* **2010**, *2010*, 1829-1832.

(9) (a) Hanada, S.; Ishida, T.; Motoyama, Y.; Nagashima, H., The Ruthenium-Catalyzed Reduction and Reductive N-Alkylation of Secondary Amides with Hydrosilanes: Practical Synthesis of Secondary and Tertiary Amines by Judicious Choice of Hydrosilanes *J. Org. Chem.* **2007**, *72*, 7551-7559. (b) Hanada, S.; Tsutsumi, E.; Motoyama, Y.; Nagashima, H., Practical Access to Amines by Platinum-Catalyzed Reduction of Carboxamides with Hydrosilanes: Synergy of Dual Si−H Groups Leads to High Efficiency and Selectivity *J. Am. Chem. Soc.* **2009**, *131*, 15032-15040. (c) Pisiewicz, S.; Junge, K.; Beller, M., Mild Hydrosilylation of Amides by Platinum N-Heterocyclic Carbene Catalysts *Eur. J. Inorg. Chem.* **2014**, *2014*, 2345-2349.

(10) (a) Iali, W.; Paglia, F. L.; Goff, X.-F. L.; Sredojević, D.; Pfeffer, M.; Djukic, J.-P., Room temperature tandem hydroamination and hydrosilation/protodesilation catalysis by a tricarbonylchromium-bound iridacycle *Chem. Commun.* **2012**, *48*, 10310-10312. (b) Corre, Y.; Iali, W.; Hamdaoui, M.; Trivelli, X.; Djukic, J. P.; Agbossou-Niedercorn, F.; Michon, C., Efficient hydrosilylation of imines using catalysts based on iridium(III) metallacycles *Catal. Sci. Technol.* **2015**, *5*, 1452-1458. (c) Michon, C.; MacIntyre, K.; Corre, Y.; Agbossou-Niedercorn, F., Pentamethylcyclopentadienyl Iridium(III) Metallacycles Applied to Homogeneous Catalysis for Fine Chemical Synthesis *Chem. Cat. Chem* **2016**, *8*, 1755-1762. (d) Corre, Y.; Rysak, V.; Nagyházi, M.; Kalocsai, D.; Trivelli, X.; Djukic, J.-P.; Agbossou-Niedercorn, F.; Michon, C., One-Pot Controlled Reduction of Conjugated Amides by Sequential Double Hydrosilylation Catalyzed by an Iridium(III) Metallacycle *Eur. J. Org. Chem.* **2020**, *2020*, 6212-6220. (e) Corre, Y.; Rysak, V.; Capet, F.; Djukic, J.-P.; Agbossou-Niedercorn, F.; Michon, C., Selective Hydrosilylation of Esters to Aldehydes Catalysed by Iridium(III) Metallacycles through Trapping of Transient Silyl Cations *Chem. Eur. J.* **2016**, *22*, 14036-14041. (f) Corre, Y.; Trivelli, X.; Capet, F.; Djukic, J.-P.; Agbossou-Niedercorn, F.; Michon, C., Efficient and Selective Hydrosilylation of Secondary and Tertiary Amides Catalyzed by an Iridium(III) Metallacycle: Development and Mechanistic Investigation *Chem. Cat. Chem* **2017**, *9*, 2009-2017. (g) Rysak, V.; Descamps-Mandine, A.; Simon, P.; Blanchard, F.; Burylo, L.; Trentesaux, M.; Vandewalle, M.; Collière, V.; Agbossou-Niedercorn, F.; Michon, C., Selective ligand-free cobalt-catalysed reduction of esters to aldehydes or alcohols *Catal. Sci. Technol.* **2018**, *8*, 3504-3512.

(11) (a) Ibrahim, A. D.; Entsminger, S. W.; Zhu, L.; Fout, A. R., A Highly Chemoselective Cobalt Catalyst for the Hydrosilylation of Alkenes using Tertiary Silanes and Hydrosiloxanes *ACS Catal.* **2016**, *6*, 3589-3593. (b) Trost, B. M.; Ball, Z. T.; Jöge, T., A Chemoselective Reduction of Alkynes to (E)-Alkenes *J. Am. Chem. Soc.* **2002**, *124*, 7922-7923.

(12) (a) Marciniec, B. *Hydrosilylation - A Comprehensive Review on Recent Advances*; Springer Science, 2009. (b) Roy, A. K. In *Advances in Organometallic Chemistry*; West, R., Hill, A. F., Fink, M.

J., Eds.; Academic Press: 2007; Vol. 55, p 1-59. (c) Hofmann, R. J.; Vlatković, M.; Wiesbrock, F., Fifty Years of Hydrosilylation in Polymer Science: A Review of Current Trends of Low-Cost Transition-Metal and Metal-Free Catalysts, Non-Thermally Triggered Hydrosilylation Reactions, and Industrial Applications *Polymers* **2017**, *9*, 534. (d) Marciniec, B.; Pietraszuk, C.; Pawluć, P.; Maciejewski, H., Inorganometallics (Transition Metal–Metalloid Complexes) and Catalysis *Chem. Rev.* **2022**, *122*, 3996-4090. (e) Asensio, J. M.; Bouzouita, D.; van Leeuwen, P. W. N. M.; Chaudret, B., σ-H–H, σ-C–H, and σ-Si–H Bond Activation Catalyzed by Metal Nanoparticles *Chem. Rev.* **2020**, *120*, 1042-1084. (f) Dobbs, A. P.; Chio, F. K. I. In *Comprehensive Organic Synthesis (Second Edition)*; Knochel, P., Ed.; Elsevier: Amsterdam, 2014, p 964-998.

(13) (a) Lipke, M. C.; Liberman-Martin, A. L.; Tilley, T. D., Electrophilic Activation of Silicon–Hydrogen Bonds in Catalytic Hydrosilations *Angew. Chem. Int. Ed.* **2017**, *56*, 2260-2294. (b) Binh, D. H.; Milovanović, M.; Puertes-Mico, J.; Hamdaoui, M.; Zarić, S. D.; Djukic, J.-P., Is the R_3Si Moiety in Metal–Silyl Complexes a Z ligand? An Answer from the Interaction Energy *Chem. Eur. J.* **2017**, *23*, 17058-17069.

(14) (a) Hamdaoui, M.; Ney, M.; Sarda, V.; Karmazin, L.; Bailly, C.; Sieffert, N.; Dohm, S.; Hansen, A.; Grimme, S.; Djukic, J.-P., Evidence of a Donor–Acceptor (Ir–H)→SiR_3 Interaction in a Trapped Ir(III) Silane Catalytic Intermediate *Organometallics* **2016**, *35*, 2207-2223. (b) Hamdaoui, M.; Desrousseaux, C.; Habbita, H.; Djukic, J.-P., Iridacycles as Catalysts for the Autotandem Conversion of Nitriles into Amines by Hydrosilylation: Experimental Investigation and Scope *Organometallics* **2017**, *36*, 4864-4882. (c) Connelly, S. J.; Kaminsky, W.; Heinekey, D. M., Structure and Solution Reactivity of (Triethylsilylium)triethylsilane Cations *Organometallics* **2013**, *32*, 7478-7481. (d) Großekappenberg, H.; Reißmann, M.; Schmidtmann, M.; Müller, T., Quantitative Assessment of the Lewis Acidity of Silylium Ions *Organometallics* **2015**, *34*, 4952-4958. (e) Klare, H. F. T.; Albers, L.; Süsse, L.; Keess, S.; Müller, T.; Oestreich, M., Silylium Ions: From Elusive Reactive Intermediates to Potent Catalysts *Chem. Rev.* **2021**, *121*, 5889-5985. (f) Kumar, N.; Laye, C.; Robert, F.; Landais, Y., Quinoline-Based Silylium Ions: Synthesis, Structure and Lewis Acidity *Eur. J. Org. Chem.* **2021**, *2021*, 3613-3621.

(15) Behzadi, M.; Gajendramurthy, C. M.; Boucher, M.; Deraedt, C.; Cornaton, Y.; Karmazin, L.; Gruber, N.; Bertani, P.; Djukic, J.-P., Electrophilic Si−H Activation by Acetonitrilo Benzo[*h*]quinoline Iridacycles: Influence of Electronic Effects in Catalysis *Chem. Eur. J.* **2023**, *29*, e202300811.

(16) Binh, D. H.; Hamdaoui, M.; Fischer-Krauser, D.; Karmazin, L.; Bailly, C.; Djukic, J.-P., Entrapment of THF-Stabilized Iridacyclic IrIII Silylenes from Double H−Si Bond Activation and H_2 Elimination *Chem. Eur. J.* **2018**, *24*, 17577-17589.

(17) (a) Mansour, T. S.; Jin, H., Synthesis of (+/−)–1′-Aza-carbocyclic-pyrimidine-2′,3′-dideoxynucleoside analogues as potential anti-HIV agents *Bioorg. Med. Chem. Lett.* **1991**, *1*, 757-760. (b) Elsanousi, A.; Riadi, Y.; Ouerghi, O.; Geesi, M. H., Synthesis, Characterization of TiO_2-Based Nanostructure as Efficient Catalyst for the Synthesis of New Heterocycles Benzothiazole-Linked Pyrrolidin-2-One: Catalytic Performances Are Particle's Size Dependent *Polycyclic Aromatic Compounds* **2023**, *43*, 2404-2417. (c) Dou, D.; He, G.; Mandadapu, S. R.; Aravapalli, S.; Kim, Y.; Chang, K.-O.; Groutas, W. C., Inhibition of noroviruses by piperazine derivatives *Bioorg. Med. Chem. Lett.* **2012**, *22*, 377-379.

(18) Arfaoui, A.; Saâdi, F.; Smida, Y. B.; Arfaoui, Y.; Nefzi, A.; Amri, H., A convenient synthesis of 3,4-cis-disubstituted pyrrolidin-2-ones *Tetrahedron Lett.* **2015**, *56*, 98-100.

(19) Mestrelab Research S.L.: Feliciano Barrera 9B, Bajo, 15706 Santiago de Compostela, Spain, 2022

(20) Bharti, S. K.; Roy, R., Quantitative ^{1}H NMR spectroscopy *TrAC Trends Anal. Chem.* **2012**, *35*, 5-26.

(21) Espenson, J. H. *Chemical Kinetics and Reaction Mechanisms*; McGraw-Hill Book Company: New York, 1981.

(22) Dai, H.-B.; Liang, Y.; Ma, L.-P.; Wang, P., New Insights into Catalytic Hydrolysis Kinetics of Sodium Borohydride from Michaelis−Menten Model *J. Phys. Chem. C* **2008**, *112*, 15886-15892.

(23) (a) Stark, J.; Görcke, M.; Arndt, M., Ermittlung des Trägers des Kontinuierlichem Spektrums der Wasserstoff-Kanalstrahlem *Annal. Phys.* **1917**, *4*, 81-110. (b) Bishop, D. M., The vibrational Stark effect *J. Chem. Phys.* **1993**, *98*, 3179-3184.

(24) (a) Pendás, A. M. n.; Blanco, M. A.; Francisco, E., Two-electron integrations in the quantum theory of atoms in molecules *J. Chem. Phys.* **2004**, *120*, 4581-4592. (b) Blanco, M. A.; Pendás, A. M.; Francisco, E., Interacting Quantum Atoms: A Correlated Energy Decomposition Scheme Based on the Quantum Theory of Atoms in Molecules *J. Chem. Theor. Comput.* **2005**, *1*, 1096-1109. (c) Francisco, E.; Martín Pendás, A.; Blanco, M. A., A Molecular Energy Decomposition Scheme for Atoms in Molecules *J. Chem. Theor. Comput.* **2006**, *2*, 90-102.

(25) (a) Lefebvre, C.; Rubez, G.; Khartabil, H.; Boisson, J.-C.; Contreras-García, J.; Hénon, E., Accurately extracting the signature of intermolecular interactions present in the NCI plot of the reduced density gradient versus electron density *Phys. Chem. Chem. Phys.* **2017**, *19*, 17928-17936. (b) Lefebvre, C.; Khartabil, H.; Boisson, J.-C.; Contreras-García, J.; Piquemal, J.-P.; Hénon, E., The Independent Gradient Model: A New Approach for Probing Strong and Weak Interactions in Molecules from Wave Function Calculations *ChemPhysChem* **2018**, *19*, 724-735. (c) Klein, J.; Khartabil, H.; Boisson, J.-C.; Contreras-García, J.; Piquemal, J.-P.; Hénon, E., New Way for Probing Bond Strength *J. Phys. Chem. A* **2020**, *124*, 1850-1860.

(26) (a) Mitoraj, M.; Michalak, A., Donor–Acceptor Properties of Ligands from the Natural Orbitals for Chemical Valence *Organometallics* **2007**, *26*, 6576-6580. (b) Mitoraj, M. P.; Michalak, A.; Ziegler, T., A Combined Charge and Energy Decomposition Scheme for Bond Analysis *J. Chem. Theor. Comput.* **2009**, *5*, 962-975.

(27) (a) Bader, R. F. W. *Atoms in Molecules: A Quantum Theory*; Oxford University Press: Oxford, 1990. (b) Bader, R. F. W., A quantum theory of molecular structure and its applications *Chem. Rev.* **1991**, *91*, 893-928.

(28) (a) Blanco, M. A.; Pendás, A. M.; Francisco, E., Interacting Quantum Atoms: A Correlated Energy Decomposition Scheme Based on the Quantum Theory of Atoms in Molecules *J. Chem. Theor. Comp.* **2005**, *1*, 1096-1109. (b) Francisco, E.; Pendás, A. M.; Blanco, M. A., A Molecular Energy Decomposition Scheme for Atoms in Molecules *J. Chem. Theor. Comp.* **2006**, *2*, 90-102.

(29) Contreras-García, J.; Johnson, E. R.; Keinan, S.; Chaudret, R.; Piquemal, J.-P.; Beratan, D. N.; Yang, W., NCIPLOT: A Program for Plotting Noncovalent Interaction Regions *J. Chem. Theor. Comp.* **2011**, *7*, 625-632.

(30) Cornaton, Y.; Djukic, J.-P., Noncovalent Interactions in Organometallic Chemistry: From Cohesion to Reactivity, a New Chapter *Acc. Chem. Res.* **2021**, *54*, 3828-3840.

(31) (a) Wu, F.; Deraedt, C.; Cornaton, Y.; Contreras-Garcia, J.; Boucher, M.; Karmazin, L.; Bailly, C.; Djukic, J.-P., Making Base-Assisted C–H Bond Activation by Cp*Co(III) Effective: A Noncovalent Interaction-Inclusive Theoretical Insight and Experimental Validation *Organometallics* **2020**, *39*, 2609-2629. (b) Cornaton, Y.; Djukic, J.-P., A noncovalent interaction insight onto the concerted metallation deprotonation mechanism *Phys. Chem. Chem. Phys.* **2019**, *21*, 20486-20498.

(32) Loir-Mongazon, L.; Antuña-Hörlein, C.; Deraedt, C.; Cornaton, Y.; Djukic, J.-P., Activation Barriers for Cobalt(IV)-Centered Reductive Elimination Correlate with Quantified Interatomic Noncovalent Interactions *Synlett* **2022**, *34*, 1169-1173.

(33) Lefebvre, C.; Klein, J.; Khartabil, H.; Boisson, J. C.; Hénon, E., IGMPlot: A program to identify, characterize, and quantify molecular interactions *J. Comput. Chem.* **2023**, *44*, 1750-1766.

(34) (a) Felluga, F.; Pitacco, G.; Prodan, M.; Pricl, S.; Visintin, M.; Valentin, E., A chemoenzymatic approach to the synthesis of

enantiomerically pure aza analogues of paraconic acid methyl ester and both enantiomers of methyl β-proline *Tetrahedron: Asym.* **2001**, *12*, 3241-3249. (b) Fujii, S.; Kawamura, H.; Watanabe, S.; organisation, E. P., Ed. 1990; Vol. EP 393607 A2 1990-10-24

(35) Campello, H. R.; Parker, J.; Perry, M.; Ryberg, P.; Gallagher, T., Asymmetric Reduction of Lactam-Based β-Aminoacrylates. Synthesis of Heterocyclic β2-Amino Acids *Org. Lett.* **2016**, *18*, 4124-4127.

(36) Besbes, R.; Villieras, M.; Amri, H., Improved synthesis and reaction of dimethyl alpha-(bromomethyl) fumarate with primary amines *Indian J. Chem.* **1997**, *36B*, 5-8.

(37) Arfaoui, A.; Saâdi, F.; Nefzi, A.; Amri, H., Easy Conversion of Dimethyl α-(Bromomethyl)fumarate into Functionalized Allyl Ethers Mediated by DABCO *Synth. Commun.* **2015**, *45*, 2627-2635.

(38) te Velde, G.; Bickelhaupt, F. M.; Baerends, E. J.; Fonseca Guerra, C.; van Gisbergen, S. J. A.; Snijders, J. G.; Ziegler, T., Chemistry with ADF *J. Comput. Chem.* **2001**, *22*, 931-967.

(39) Perdew, J. P.; Burke, K.; Ernzerhof, M., Generalized Gradient Approximation Made Simple *Phys. Rev. Lett.* **1996**, *77*, 3865-3868.

(40) Caldeweyher, E.; Ehlert, S.; Hansen, A.; Neugebauer, H.; Spicher, S.; Bannwarth, C.; Grimme, S., A generally applicable atomic-charge dependent London dispersion correction *J. Chem. Phys.* **2019**, *150*, 154122.

(41) (a) vanLenthe, E.; Baerends, E. J.; Snijers, J. G., Relativistic regular two-component Hamiltonians *J. Chem. Phys.* **1993**, *99*, 4597-4610. (b) vanLenthe, E.; Baerends, E. J.; Snijders, J. G., Relativistic total energy using regular approximations *J. Chem. Phys.* **1994**, *101*, 9783-9792. (c) Lenthe, E. v.; Ehlers, A.; Baerends, E. J., Geometry optimizations in the zero order regular approximation for relativistic effects *J. Chem. Phys.* **1999**, *110*, 8943-8953.

(42) (a) Klamt, A.; Schüürmann, G., COSMO: a new approach to dielectric screening in solvent with explicit expressions for the screening energy and its gradient. *J. Chem. Soc., Perkin Trans.2* **1993**, 799-805. (b) Klamt, A., Conductor-like Screening Model for real solvents: a new approach to the quantitative calculation of solvation phenomena. *J. Phys. Chem.* **1995**, *99*, 2224-2235. (c) Klamt, A.; Jonas, V., Treatment of the outlying charge in continuum solvation models. *J. Chem. Phys.* **1996**, *105*, 9972-9981.

(43) Franchini, M.; Philipsen, P. H. T.; Visscher, L., The Becke fuzzy cells integration scheme in the Amsterdam Density Functional program suite. *J. Comput. Chem.* **2013**, *34*, 1819-1827.

(44) (a) Deng, L.; Ziegler, T., Reaction path following in mass-weighted internal corrdinates *Int. J. Quantum Chem.* **1990**, *94*, 5523-5527. (b) Deng, L.; Ziegler, T.; Fan, L., A combined density functional and intrinsic reaction coordinate study on the ground state energy surface of H_2CO *J. Chem. Phys.* **1993**, *99*, 3823.

(45) (a) Grimme, S.; Antony, J.; Ehrlich, S.; Krieg, H., A consistent and accurate ab initio parametrization of density functional dispersion correction (DFT-D) for the 94 elements H-Pu *J. Chem. Phys.* **2010**, *132*, 154104. (b) Grimme, S.; Ehrlich, S.; Goerigk, L., Effect of the damping function in dispersion corrected density functional theory *J. Comput. Chem.* **2011**, *32*, 1456-1465.

(46) Weigend, F.; Ahlrichs, R., Balanced basis sets of split valence, triple zeta valence and quadruple zeta valence quality for H to Rn: Design and assessment of accuracy *Phys. Chem. Chem. Phys.* **2005**, *7*, 3297-3305.

(47) Marenich, A. V.; Cramer, C. J.; Truhlar, D. G., Universal Solvation Model Based on Solute Electron Density and on a Continuum Model of the Solvent Defined by the Bulk Dielectric Constant and Atomic Surface Tensions *J. Phys. Chem. B* **2009**, *113*, 6378-6396.

(48) Neese, F., The ORCA program system. *WIREs Comput. Mol. Sci.* **2012**, *2*, 73-78.

Table of content graphical abstract